AD NUMBER

AD863260

NEW LIMITATION CHANGE

TO

Approved for public release, distribution unlimited

FROM

Distribution authorized to U.S. Gov't. agencies and their contractors; Critical Technology; AUG 1969. Other requests shall be referred to Air Force Aero Propulsion Laboratory, Attn: APRT, Wright-Patterson AFB, OH 45433.

AUTHORITY

AFWAL ltr, 22 Dec 1983

AFAPL-TR-69-82

INVESTIGATION OF THE IGNITION PROPERTIES OF FLOWING COMBUSTIBLE GAS MIXTURES

Darrell W. Walker
Larry A. Diehl
William A. Strauss
Rudolph Edse

The Ohio State University
Columbus, Ohio

September 1969

Contract F33615-68-C-1580

Air Force Aero Propulsion Laboratory
Air Force Systems Command
United States Air Force
Wright-Patterson Air Force Base, Ohio

FOREWORD

This report was prepared by W. A. Strauss, D. W. Walker, L. A. Diehl, and R. Edse, of the Department of Aeronautical and Astronautical Engineering of The Ohio State University on Contract No. F33615-68-C-1580, "Investigation of the Conditions Leading to Spontaneous Ignition in Flowing Explosive Gas Mixtures." The work on this task was administered under the direction of the Air Force Aero Propulsion Laboratory (AFSC), Ramjet Engine Division, Wright-Patterson Air Force Base, Ohio, with Mr. W. Lee Bain as Project Engineer.

This technical report covers the research conducted on Contract No. F33615-68-C-1580 during the period 15 April 1968 through 14 July 1969. Publication of this report does not constitute Air Force approval of the report's findings or conclusions. It is published only for the exchange and stimulation of ideas.

W. LEE BAIN
Project Engineer
Air Force Aero Propulsion Laboratory
Wright-Patterson AFB, Ohio 45433

ABSTRACT

Ignition delay times, ignition temperatures, and spontaneous ignitions were determined for several combustible gas mixtures behind incident and reflected shock waves passed into the static or flowing gases.

The conditions leading to spontaneous ignition of flowing hydrogen-oxygen mixtures without the presence of shock waves were also determined. Hydrogen air mixture did not ignite spontaneously under the range of experiments conducted.

Although certain observations indicate that the spontaneous ignition can be produced by aerodynamic heating, it must be assumed that other phenomena could also cause these ignitions. The observed high temperatures in the resonating gases should have been sufficient to ignite the hydrogen-air mixtures.

While the ignition temperature and ignition delay time of methane-air and ethylene-air mixtures do not depend on the motion of the unburned gas mixture, those of hydrogen-air mixtures were much lower behind incident than behind reflected shock waves.

A brief discussion of the mechanism of ignition under the various conditions is included.

TABLE OF CONTENTS

LIST OF FIGURES

LIST OF FIGURES - (Continued)

LIST OF TABLES

LIST OF SYMBOLS

F	frequency
M	Mach number
$\dot{m}$	mass flow
P	pressure
T	temperature
t	time
U	particle speed
η	mole fraction
τ	ignition delay time
$[O_2]$	concentration of O_2 species
$\%H_2$	mole percent of hydrogen species in mixture

Subscripts

i	preshock gas conditions
ig	conditions at ignition of mixture
i,in	preshock gas flow conditions at inlet of flow tube (Fig. 2)
i,x	preshock gas flow conditions 6.4 cm before exit of flow tube (Fig. 2)
RC	fuel line chamber resonance conditions (Fig. 3)
r	reflected shock conditions
p	oxidizer line chamber conditions (Fig. 3)
W	wave
0	stagnation in conditions
1	initial gas conditions in conventional shock tube
2	conditions behind incident shockwave

I. INTRODUCTION

The performance of a hypersonic ramjet engine is best when the flow of gas in the combustor is supersonic at all times.[1] Fuels presently being considered for the scramjet engine are hydrogen and the lower molecular weight hydrocarbons. The ignition properties of the various fuel-air mixtures at supersonic speeds are of considerable importance to the design of this type combustor. In the first part of the present study, the minimum ignition temperatures and the ignition delay times of potential scramjet propellants were measured as a function of mixture ratio, gas velocity, and pressure. The second phase of this study deals with the autoignition of flowing fuel-oxidizer mixtures. The latter phenomenon represents a serious safety hazard when flowing combustible mixtures are employed.

The minimum ignition temperatures of fuel-air mixtures may be calculated from the thermal explosion limit theory.[2] However, available experimental data on the minimum ignition temperatures of various fuel-oxidizer mixtures indicate that this theory is generally not valid.[3] The actual ignition temperatures depend greatly on the technique used to heat the gas mixtures (shocks, external heat addition) and on the initial pressure of the combustible gas mixture. For methane-oxygen mixtures, Shepherd[4] gave the minimum ignition temperature as 920°K (using incident shock waves) while Kane and associates[5] reported a value of 840°K; they used a reaction chamber. Fay[6] and Belles[3] measured the minimum ignition temperatures of hydrogen-oxygen mixtures behind incident shock waves and reported values of 630°K and 780°K, respectively. Belles also determined the minimum ignition temperature of a stoichiometric hydrogen-air mixture and reported a value of 630°K (which is 150°K below the value calculated from the explosion limit theory). Craig,[7] in a study on the effect of additives on the ignition delay times of hydrogen-air mixtures, found the minimum ignition temperature to be 440°K. He employed incident shock waves to heat the combustible gas mixtures. However, ignition occurred behind reflected shock waves only when the mixtures exceeded temperatures of 880°K at the same final pressure. The latter author attributed this discrepency to contamination of the mixture by loose deposits on the inside wall of the shock tube.

The ignition delay times of hydrogen-air and various hydrocarbon-air mixtures as a function of temperature behind reflected shock waves have been reported by various authors.[8-12] Montchiloff[8] and Nicholls[12] conducted a theoretical investigation of the effect of nitrogen gas on the ignition delay times of hydrogen-oxygen mixtures. They concluded that it has practically no effect on the ignition delay times; this result also agrees with experimental data. Data on the ignition delay times of static methane-air mixtures are generally not available in the literature.

The conditions behind shock waves driven into flowing combustible gas mixtures are of great practical importance because of the potential application of the detonative combustion mode in hypersonic ramjet combustors. McKenna[13] measured detonation wave speeds in flowing (subsonic and supersonic) hydrogen-oxygen mixtures. Hamilton[14] determined the shock ignition characteristics of flowing (subsonic) hydrogen-oxygen mixtures. In the latter study, it was reported that the shock strength required to produce ignition of the mixture decreased with increasing Mach number of the gas flow. Preliminary experiments with flowing fuel-oxidizer mixtures at this laboratory revealed that autoignitions of these mixtures can occur even when the total temperature of the flowing mixture is far below the established minimum ignition temperature of the mixture. In his investigation of the propagation of detonation waves through flowing combustible gas mixtures, McKenna reported "accidental detonations" which were initiated at various positions along the tube for both supersonic as well as subsonic gas flows. Bollinger et al.[15] reported similar phenomena for hydrogen-oxygen mixtures but at much lower flow velocities. The latter authors suggested that the autoignitions resulted from a catalytic reaction caused by the pyrofuse ignition. In a study of the combustion of hydrogen-air mixtures in a supersonic flowstream, Tamagno et al.[16] reported that ignition of the mixtures occurred at temperatures well below the accepted minimum autoignition temperature of the mixture.

Since flowing explosive gas mixtures are used in the study of supersonic combustion problems, it is imperative that the conditions of autoignition be thoroughly understood. It was the basic purpose of this investigation to study the ignition properties and autoignition characteristics of flowing hydrogen-air and flowing hydrocarbon-air mixtures. From a practical point of view these studies are of great importance because it can be expected that the results will have a great influence on the design of ramjet combustors.

II. APPARATUS, INSTRUMENTATION, AND METHOD

The investigation consists of three separate studies, each of which required different experimental apparatus and instrumentation. A conventional shock tube apparatus was employed to measure the minimum ignition temperatures and ignition delay times in static fuel-air mixtures behind reflected shock waves. Another shock tube apparatus was used to measure the minimum ignition temperatures and the ignition delay times of flowing fuel-air mixtures. In this case, shock waves were driven into the flowing mixtures. A third experimental apparatus was used to study the autoignition properties of fuel-oxidizer mixtures without assistance from a shock tube. The details of these experimental set-ups, and the corresponding instrumentation and operation are discussed in separate paragraphs below.

A. CONVENTIONAL SHOCK TUBE APPARATUS

Figure 1 is a sketch of the conventional shock tube apparatus and instrumentation used for the measurements of the ignition temperatures and delay time of fuel-air mixtures behind reflected shock waves. The driver and driven sections of the tube have an inside diameter of 8.4 cm and are 3.5 and 5.8 meters long, respectively. Mylar burst diaphragms served to separate the driver and driven sections. Helium - N_2 - Ar gas mixtures were used as the driver gas. The fuel-air mixtures being investigated were prepared in a high-pressure vessel. This vessel was pressurized first with the oxidizer and then with the fuel to provide the desired fuel-to-oxidizer mass ratio (perfect gas conditions were assumed to apply). After both gases were introduced into the cylinder the gases were mixed with a paddle wheel agitator. The initial pressures of the driven gas were selected to produce the desired pressure behind the incident shock (or reflected shock). All initial pressures were measured with Wallace and Tiernan absolute pressure gages. The conditions of temperature and pressure behind the shock wave were calculated by means of the normal shock relations with the measured incident shock speeds. The arrival of the incident shock wave was indicated by platinum strip thermal gages which were separated by a known distance. From the times (measured with the aid of an oscilloscope) required for the shock to traverse the distance between the two probes the shock speeds were easily determined. Ignition of the mixtures was ascertained by monitoring the radiation from the flames with an RCA 1P28 photomultiplier tube. Ignition delay times were determined (detected by a platinum strip thermal gage) and passage of the combustion wave past the same location (as detected by a photomultiplier tube).

B. APPARATUS FOR DRIVING A SHOCK WAVE INTO FLOWING GAS

Figure 2 is a sketch of the apparatus to study the minimum ignition temperatures and ignition delay times of flowing combustible gas mixtures. The system consists of a flow-metering and flow-control apparatus, a mixing chamber, a flow nozzle, a flowing gas tube, and a shock tube assembly.

The fuel and oxidizer flow rates were metered with sharp-edged, flat-plate orifice flow meters. The flow meters were of the "pipe tap design" and conformed to the American Gas Association (AGA) and American Society of Mechanical Engineers (ASME) standards.[17] The nominal inside diameter of the tubes was 5.0 cm. The gas pressure in the meters was regulated with Grove Dome pressure regulators, while the mass flow through the system was throttled by means of Annin control valves. The pressure drop across the flat-plate orifice was measured with a Barton differential pressure indicator, while the gas pressure was measured by a Bourdon pressure gage.

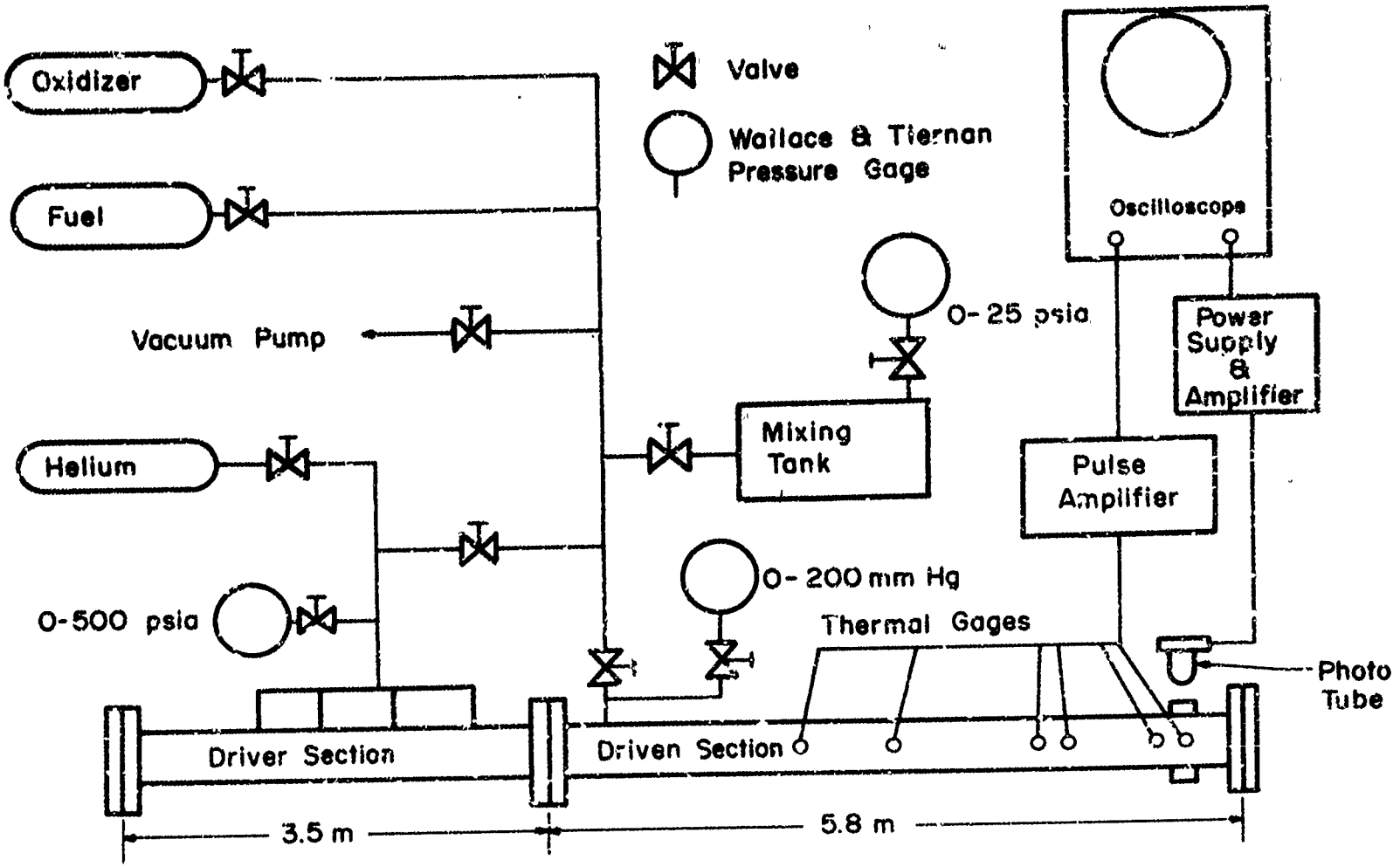

Figure 1 - Conventional Shock Tube Apparatus

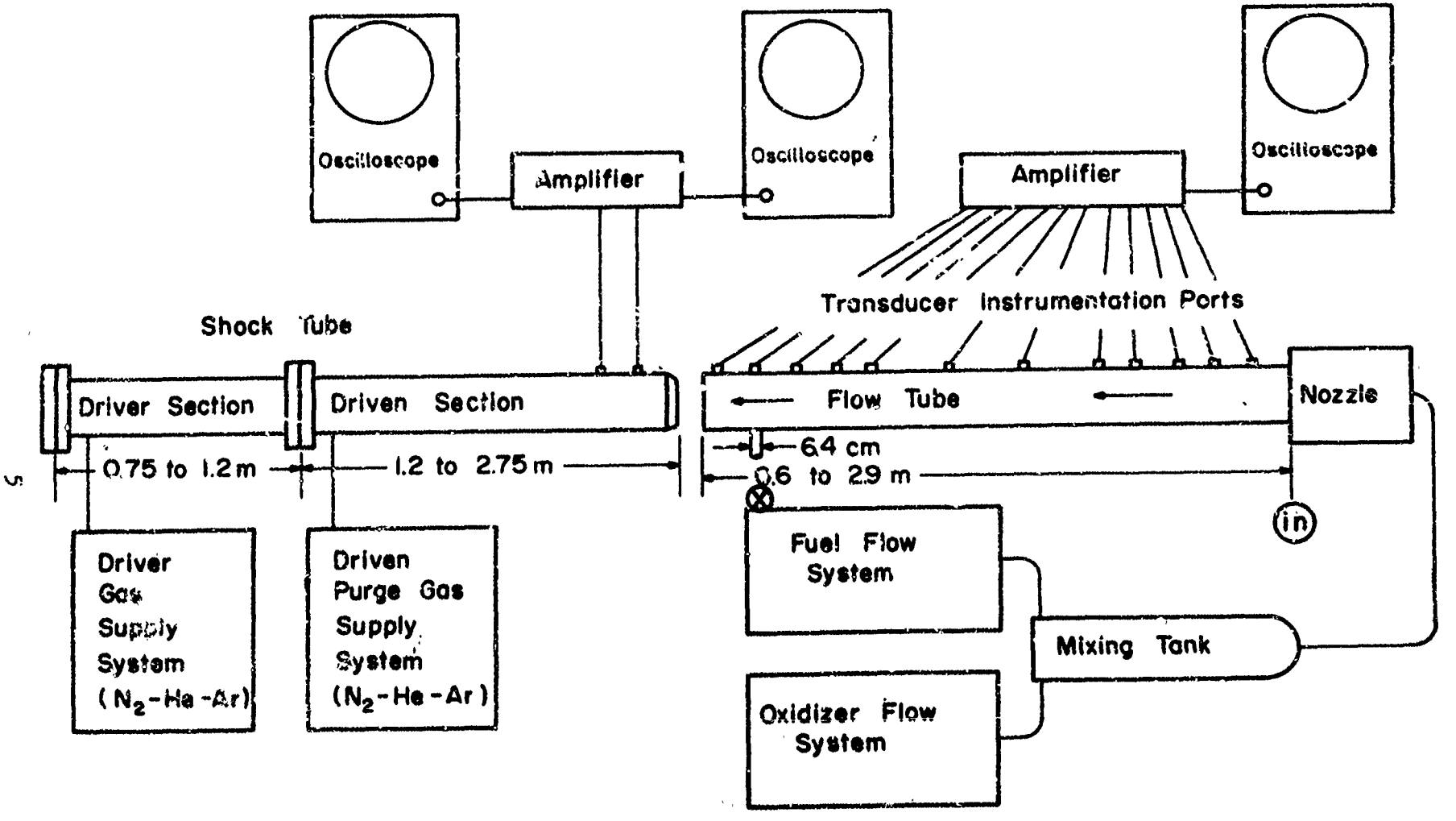

Figure 2 - Apparatus to Shock Initially Flowing Gas Mixtures

The nozzle assembly was used to produce the desired Mach numbers of the flows of the combustible gas mixtures in the flow tube. The channel through which these flows were passed consisted of a housing capable of holding various axisymmetric nozzles for supersonic and subsonic operation. These nozzles were made of copper to reduce the possibility of burnout when the combustible mixtures ignited.

Three different length flow-tube sections were used in this study. The lengths of the tubes depended on the desired Mach number (from Fanno flow theory[18]) and the characteristics of the combustible mixture being studied. The lengths of the three sections used were 2.9, 2.1, and 0.6 meters. The flow tubes were constructed from stainless steel tubes having an inside diameter of 4.25 cm and an outside diameter of 5.0 cm. This particular inside diameter was selected since it is close to the tube diameters of other researchers making similar studies. Moreover, it was reported by Bollinger[19] that sizes smaller than this value can have significant wall effects. The inside surface of the tube was polished to avoid disturbances of the gas flow.

Pressure transducers and heat transfer gages were used to measure the speed of the shock wave at different positions in the flow tube. The probes were located to permit measurements of the shock speed at the exit of the flow tube as well as at various upstream positions. The former probe position was used primarily for the minimum ignition temperature studies while the latter positions were used primarily for the ignition delay time studies. Ionization probes were used to detect the point at which ignition of the mixtures occurred and to measure the speed of the combustion wave. The times required for the waves to traverse the distance between the probes were obtained from oscilloscope traces in the usual manner.

The Mach number of the gas flow at various positions along the flow tube was determined from pressure measurements at the inlet, the center, and the exit of the flow tube.

The inner diameter of the shock tube was the same as that of the flow tube. For the experiments with hydrogen-air mixtures the shock tube consisted of a 0.75-meter driver section and a 1.2-meter driven section. Measurements in methane-air and ethylene-air mixtures were made with a shock tube having a 1.22-meter driver section and two driven sections 2.0 and 2.75 meters long. The increased length of the shock tube for the latter systems was necessary because these systems have longer ignition delay times and therefore require greater test times. Hydrogen or helium gases were used as driver gas (depending on the shocked-gas temperatures required). Mylar diaphragms were used for the lower shocked-gas temperatures, while scored aluminum diaphragms were used for the higher temperatures. Air was used as the buffer gas in the driver section of the shock tube for the hydrogen-air and ethylene-air experiments. Nitrogen gas was used as the buffer in the driven section of the shock tube for the methane-air experiments since the

shocked-gas temperatures for this study were very high and ignition of the hydrogen driver and air buffer could occur. A thin aluminum foil diaphragm was placed over the exit of the shock tube to prevent the flowing combustible gas mixture from diffusing into the driven section of the shock tube.

The experimental data collected for the ignition temperatures and ignition delay times in flowing mixtures included the time increments required for the shock or combustion wave to travel between the sensing probes (ionization gages, platinum strip thermal gages, and Kistler piezoelectric pressure transducers). The times were measured with two Tektronix Storage Oscilloscopes (Type 564) and a Dual Beam Tektronix Oscilloscope (Type 555) in the usual manner.

The procedure used to conduct the experiments for measuring the minimum ignition temperature and the ignition delay time follows. The fuel and oxidizer gas flows are adjusted to the proper values to produce the desired fuel-oxidizer mixture ratio, mass flow, and Mach number at the exit of the flow tube. The driver section of the shock tube is pressurized until the diaphragm separating the driver and driven section ruptures (breaking pressure is dependent on the diaphragm thickness). The shock wave moves through the driven section of the shock tube and breaks the thin aluminum foil at the exit of the shock tube. The shock wave then traverses the space between the shock tube exit and the exit of the flow tube (maximum distance = 5.0 cm for the M = 1.8 flow). The shock wave then passes through the flowing gas mixture in the flow tube. The speed of the wave in the flow tube is measured by the sensing probes. The ignition delay times are measured in a manner similar to that described in Part A of this section of the report.

C. AUTOIGNITION APPARATUS

The flow control and metering equipment was essentially the same as that used for the determination of the ignition properties of flowing gas mixtures (described in Part B of this section). Figure 3 shows the arrangement which was used to test the flowing mixtures for autoignition. The design consisted of individual fuel and oxidizer inlets at the base of the mixture tube. The basic inlet configuration is depicted in Figure 3a while alternate configurations are depicted schematically in Fig. 3b-3e. The fuel and oxidizer inlet tubes were 0.8 cm inside diameter (stainless steel) while the mixing tube was 2.25 cm inside diameter (also stainless). The length of the mixing tube was varied from 6.3 to 50.0 cm.

An apparatus was designed to indicate the presence of electrically charged particles in the flowing combustible gas mixtures. This apparatus was similar to the basic flow configuration equipment (Fig. 3a) and had a mixing tube length of 61 cm. The charge sensing device consisted

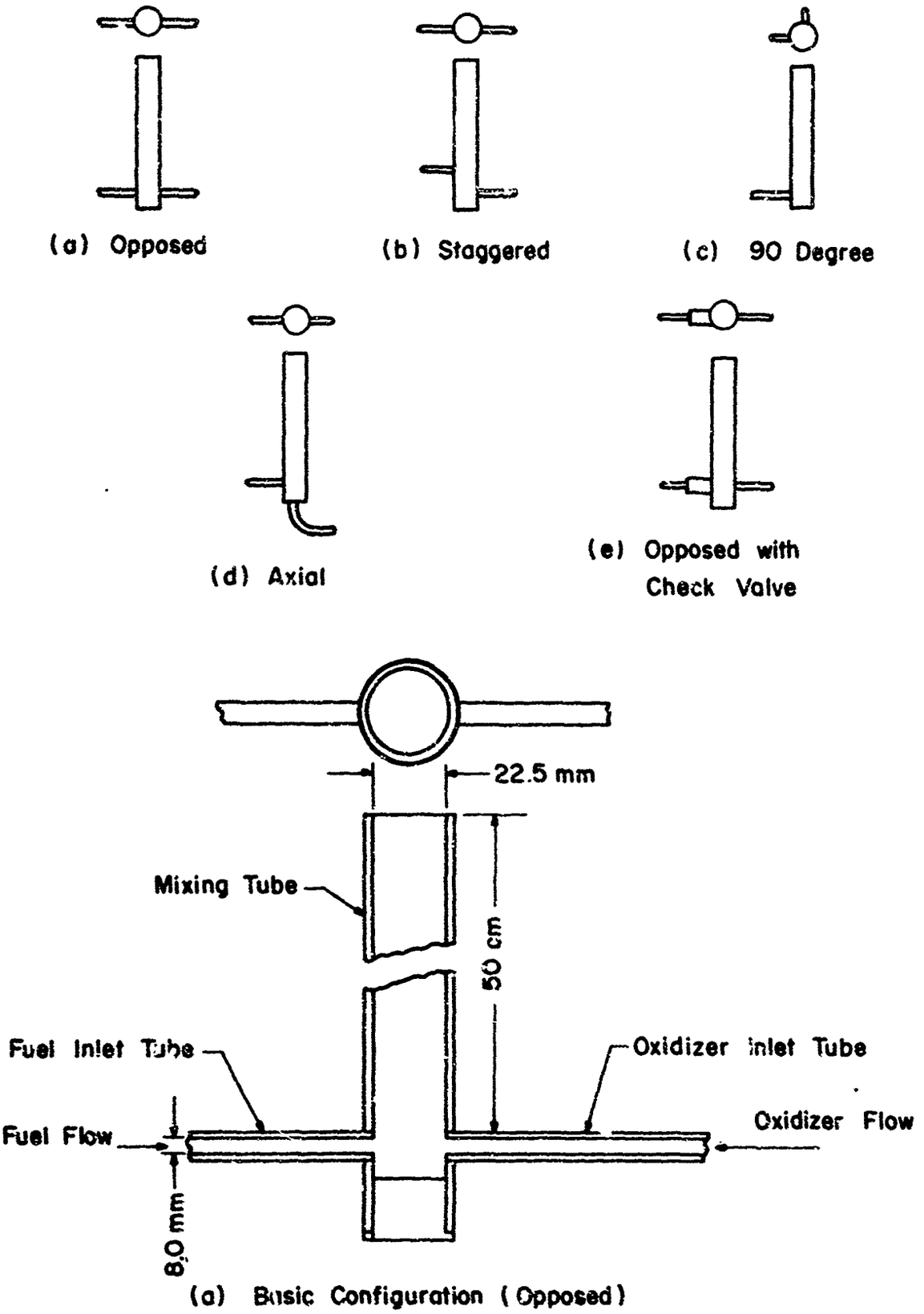

Figure 3 - Apparatus for the Study of Spontaneous Ignitions in Flowing Fuel-Oxidizer Mixtures

of (1) an electrostatic probe and (2) a pair of electrostatically charged plates.

The experiments were conducted by first stabilizing the oxidizer (air or oxygen) and then adding the fuel (hydrogen). A wide range of fuel and oxidizer flow rates were checked to establish the autoignition characteristics with the various tube designs. The charge detection experiments were conducted with nonpremixed gases to avoid damage in case of autoignition. Thermocouples and piezoelectric pressure transducers were used to measure the temperature and pressure variations within the feed lines and mixture tube.

III. RESULTS

The various investigations were carried out with commercial gases. The sources and the manufacturers' analyses of these gases are listed in Appendix I. The initial conditions of the flowing mixtures were determined from nozzle theory and Fanno flow theory.[18] The conditions of the shocked gas were calculated from normal shock theory and from measurements of the shock speed. The shock tube and the flow tube were separated (Fig. 2) a distance such that the end of the shock tube did not affect the gas conditions (pressure, Mach number, etc.) at the exit of the flow tube. To correctly evaluate the conditions of the gases behind the shock wave as it passed into the flow tube, it was necessary to know the nature and the form of the shock wave as it passed through the gap between the two tubes. Schlieren stop-action photographs were taken of typical strength shock waves as they passed through the gap into varying gas flows. The speed of the shock wave leaving the shock tube was approximately 700 m/sec. Figures 4, 5, 6, and 7 show the nature of the shock for gas flow Mach numbers of 0.0, 0.36, 0.94, and 1.8, respectively. The gap distances for the various flow cases are given in the figures. For the propagation of a normal shock wave into static air (M = 0, Fig. 4), the normal shock surface at the axis of the system decreases in size and the wave becomes completely spherical after traveling a distance of approximately 5 cm. For the M = 0 experiments, however, no air gap was necessary and it can be expected that the shock is normal in the driven section. For the flowing gas cases, it is seen from Figs. 5-7 that the shock wave traverses the gap between the two tubes in an essentially normal fashion. It can, therefore, be expected that the shock wave in the flow tube is also normal. Of course, losses at the gap will decrease the shock strength. The latter, however, is of no particular significance since the shock speeds were measured in the flow tube. Measurements showed that the decrease in shock speeds for the system with a tube gap were about the same as those without a gap. For the Mach 0.36 and 0.94 cases, there is some evidence that the gases are resonating in the gap region.

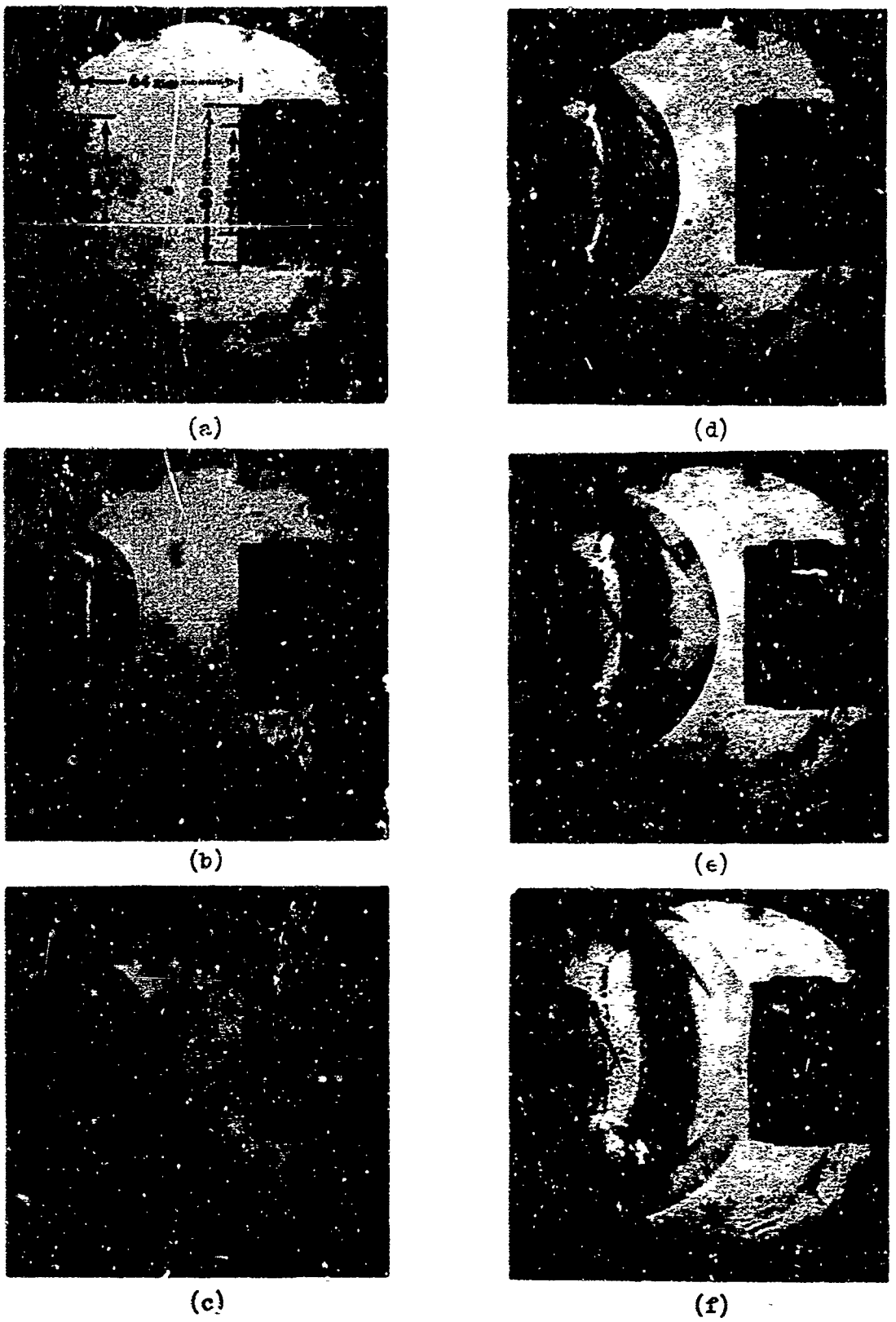

Figure 4 - Shock Wave Passing from a Shock Tube into Free Space

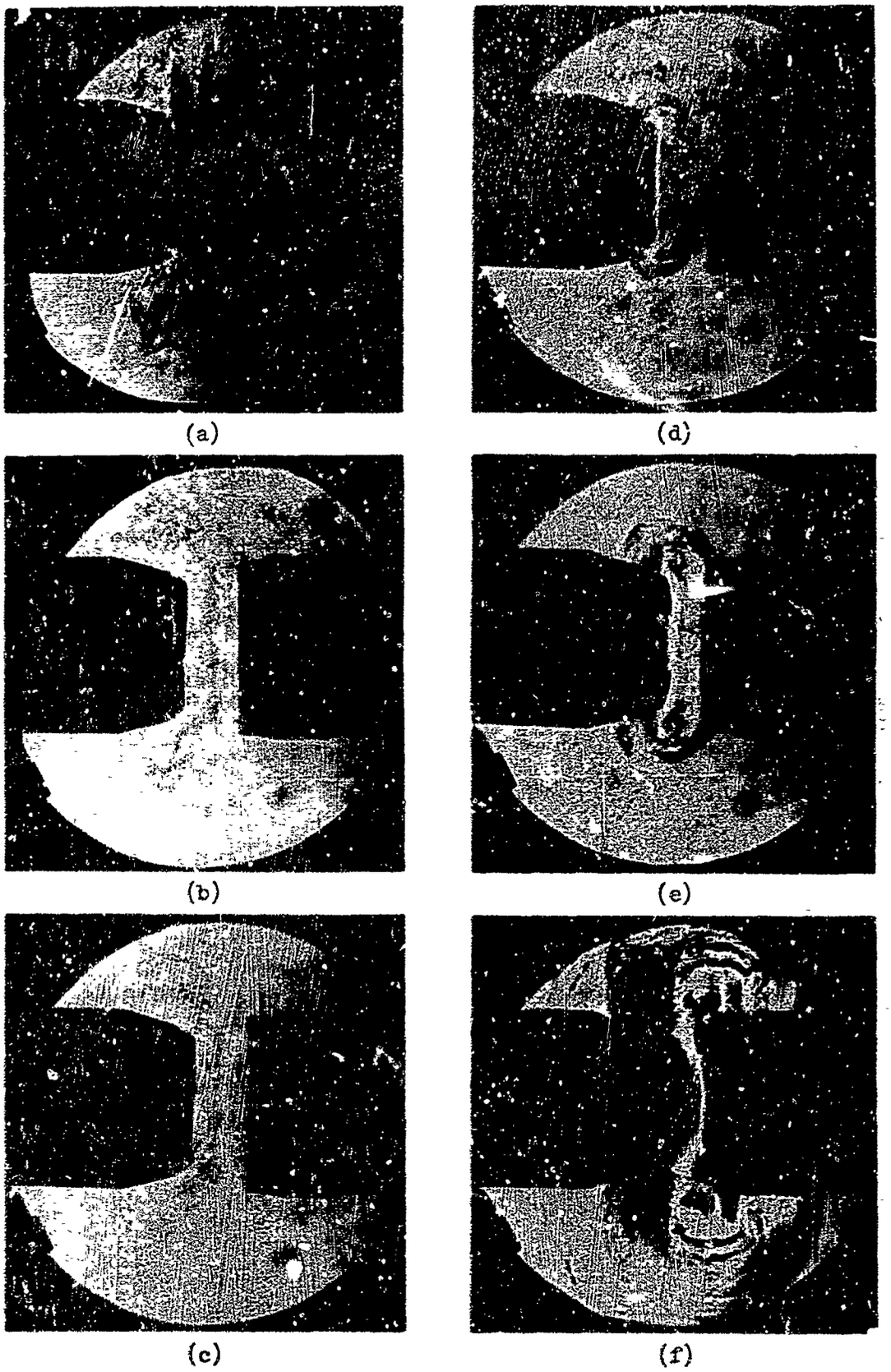

Figure 5 - Shock Wave Passing from a Shock Tube into a M = 0.36 Airflow

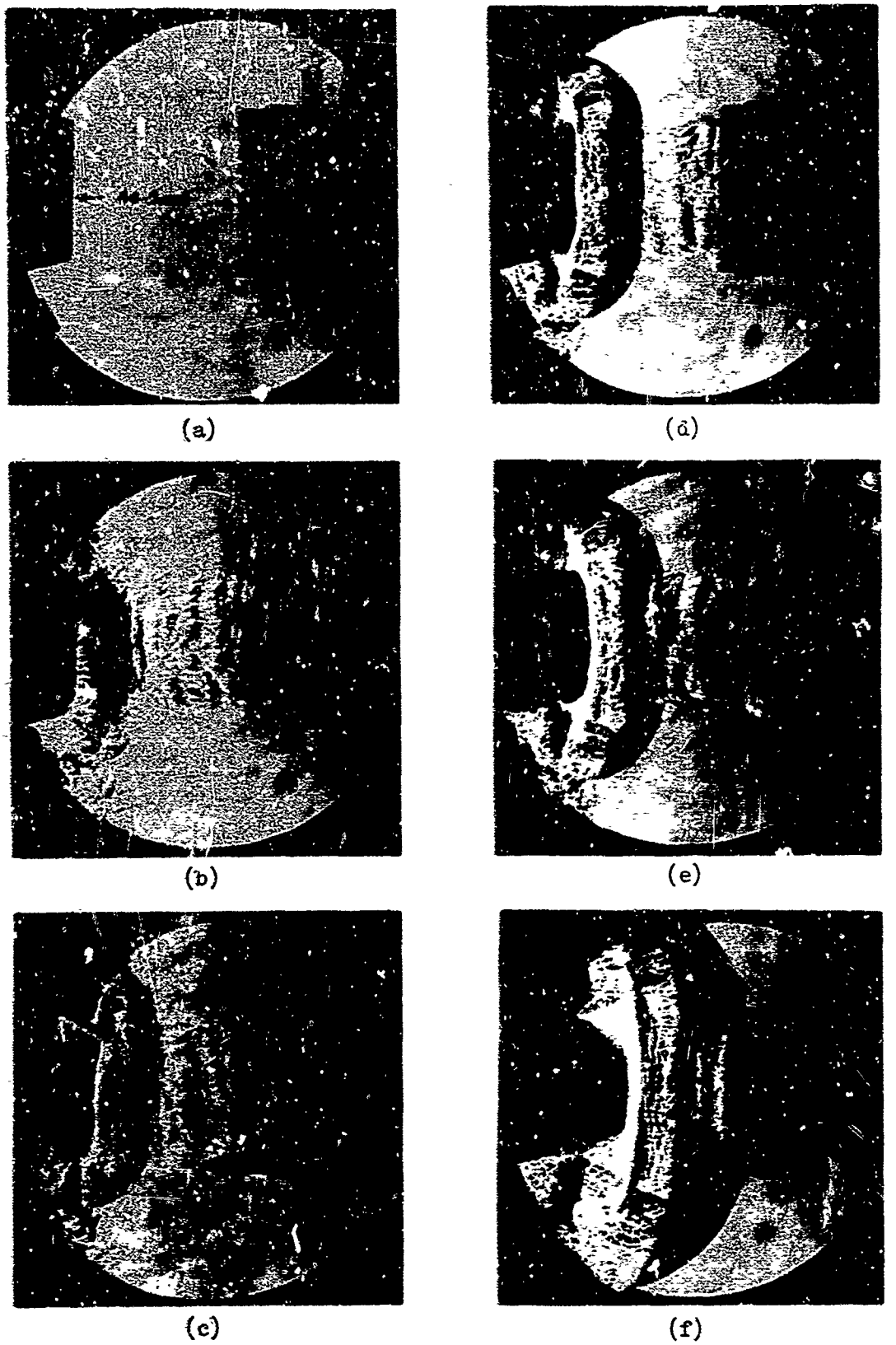

Figure 6 - Shock Wave Passing from a Shock Tube into a M = 0.94 Airflow

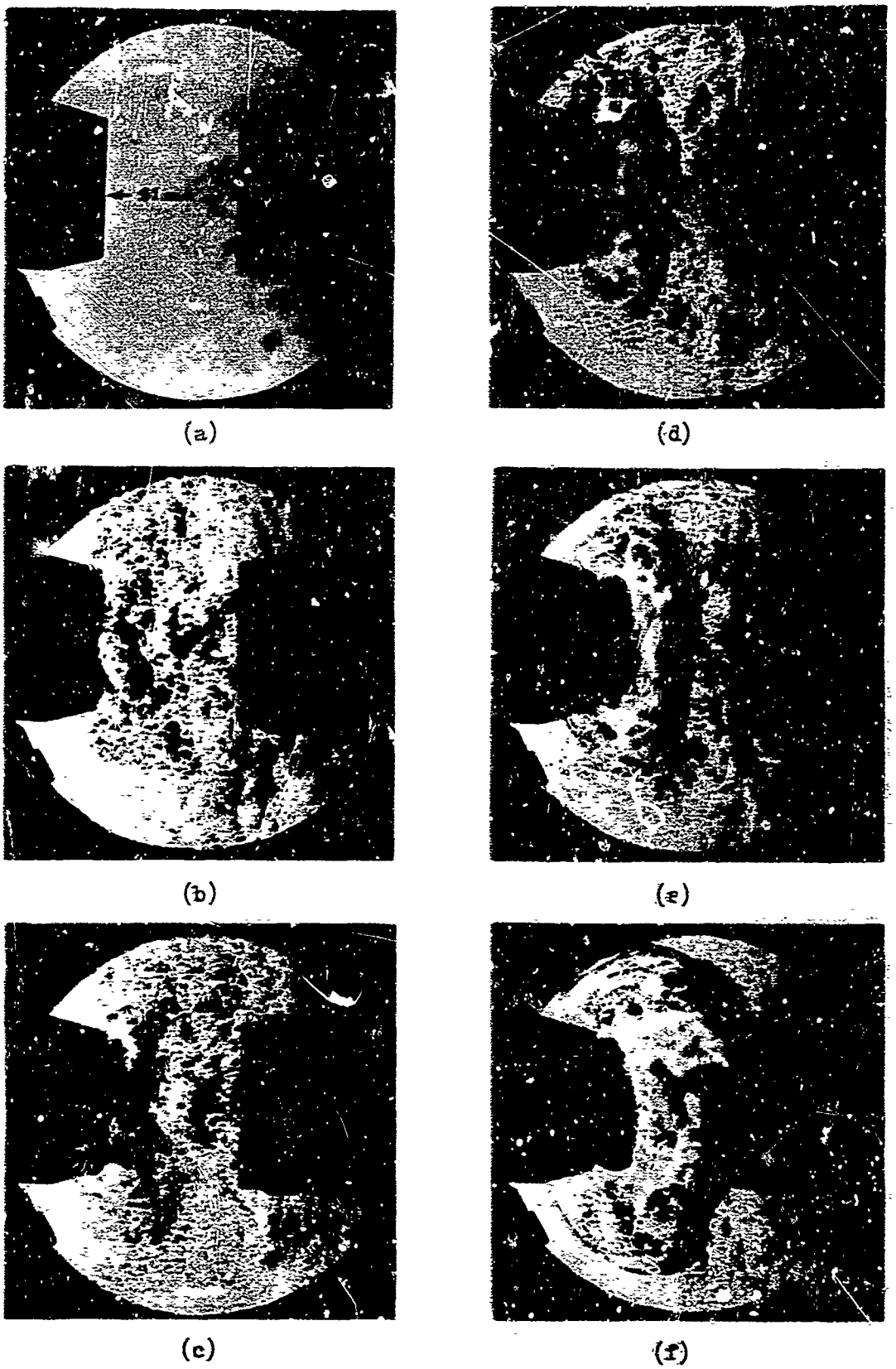

Figure 7 -- Shock Wave Passing from a Shock Tube into a M = 1.6 Airflow

A. SHOCK IGNITION TEMPERATURES

The minimum shock ignition temperatures of various flowing fuel-air mixtures are tabulated in Tables I, II, and III. The minimum ignition temperatures of flowing stoichiometric methane-air and stoichiometric ethylene-air mixtures at 15 atm pressure are approximately 940°K and 740°K, respectively. A study of the pressure dependence of the ignition temperature of static stoichiometric methane-air mixtures was made. The results of this investigation are plotted in Fig. 8 and tabulated in Table II.

Results of the minimum ignition temperature measurements as a function of initial flow Mach number for various hydrogen-air mixtures are plotted in Fig. 9 and tabulated in Table I. These data indicate that over the pressure range studied the minimum ignition temperature is dependent on the particle speed. The effect of pressure on the static ignition temperature of the stoichiometric hydrogen-air mixture was also studied and the results are tabulated in Table I and plotted in Fig. 10.

B. IGNITION DELAY TIMES

The products of the ignition delay time and the oxygen gas concentration of the stoichiometric hydrogen-air, the stoichiometric methane-air, and the stoichiometric ethylene-air mixtures for various temperatures are plotted in Fig. 11, 12, and 13 and tabulated in Tables IV, V, and VI, respectively. These data include the ignition delay times of both flowing as well as static mixtures. As can be seen from these figures, the ignition delay times of the methane-air and the ethylene-air mixtures are dependent only on the static temperature and the oxygen gas concentration. Equations of lines representing mean square fits of the data points are given in the figures. Scatter of the data points is believed to be caused by flame spinning which is known to occur for low-temperature burning. Ignition delay times of hydrogen-air mixtures were also observed at temperatures below 850°K for flowing mixtures. These temperatures are below the minimum ignition temperature of static hydrogen-air mixtures.

C. AUTOIGNITION EXPERIMENTS

Spontaneous ignitions of flowing hydrogen-oxygen mixtures were investigated for a variety of flow rates, and inlet geometries. A systematic study of the autoignition phenomenon of this mixture was undertaken with the apparatus shown in Fig. 3. To avoid the accumulation of large amounts of unburned fuel and oxidizer in the test bay, the oxidizer flow was always established first and, thereafter, the fuel was added. Inlet configurations other than the diametrically opposed case (offset and radial variations, shown in Figs. 3b-d)

Table I - Shock Ignition Temperatures of Hydrogen-Air Mixtures

M_i	% H_2	T_{ig}(°K)	T_{o2}(°K)	P_2(atm)	U_2(mps)	M_2	M_w	T_i(°K)
Flow System Data								
0.0	29.6	538.6	659.5	5.32	585.0	1.068	2.21	288.0
0.36	29.6	534.7	595.0	5.08	422.8	0.775	2.15	295.1
0.94	18.4	783.7	908.0	13.58	563.0	0.902	3.29	257.8
0.94	25.0	621.8	680.0	9.55	386.7	0.667	2.75	259.8
0.94	29.6	601.1	652.0	9.00	375.4	0.650	2.69	257.8
0.94	45.0	605.0	656.0	9.70	424.8	0.648	2.705	257.7
1.78	25.0	774.7	844.0	7.71	437.3	0.685	4.039	188.5
1.83	29.6	757.0	818.0	7.80	427.9	0.659	4.048	184.0
1.76	33.6	705.5	746.0	6.87	412.1	0.652	3.76	180.0
1.72	45.0	684.4	734.5	6.75	419.6	0.610	3.726	188.3

P_1 (mm Hg)	% H_2	T_{ig}(°K)	P_2(mm Hg)
Conventional Shock Tube Data			
50.0	29.6	700.0	417
190.0	29.6	640.0	1370
517.0	29.6	570.0	2845
P_1(mm Hg)	% H_2	T_{ig}(°K)	P_r(mm Hg)
Conventional Shock Tube Data			
50.0	29.6	800.0	910
100.0	29.6	800.0	1830
160.0	29.6	800.0	3040
200.0	29.6	860.0	4520
375.0	29.6	850.0	7910

Table II - Shock Ignition Temperatures of Stoichiometric Methane-Air Mixtures

M_i	T_{ig}(°K)	T_{o2}(°K)	P_2(atm)	U_2(mps)	M_2	M_w	T_i(°K)
Flow System Data							
0.33	943.0	1200.0	16.12	898.0	1.453	3.80	272.4
0.90	923.7	1162.0	19.92	743.4	1.214	4.08	243.3

P_1(mm Hg)	P_r(atm)	T_{ig}(°K)
Conventional Shock Tube Data		
30.0	1.735	1100.0
40.0	2.095	1100.0
60.0	3.00	1100.0
120.0	7.55	1115.0
280.0	13.4	1015.0
350.0	15.2	960.0

Table III - Shock Ignition Temperatures of Stoichiometric Ethylene-Air Mixtures

M_i	T_{ig}(°K)	T_{o2}(°K)	P_2(atm)	U_2(mps)	M_2	M_w	T_i(°K)
Flow System Data							
0.33	747.6	967.0	11.62	699.4	1.298	3.20	277.9
0.90	746.0	892.0	15.03	570.7	1.053	3.51	244.3

P_1(mm Hg)	P_r(atm)	T_{ig}(°K)
Conventional Shock Tube Data		
30	1.075	915
300	6.70	730

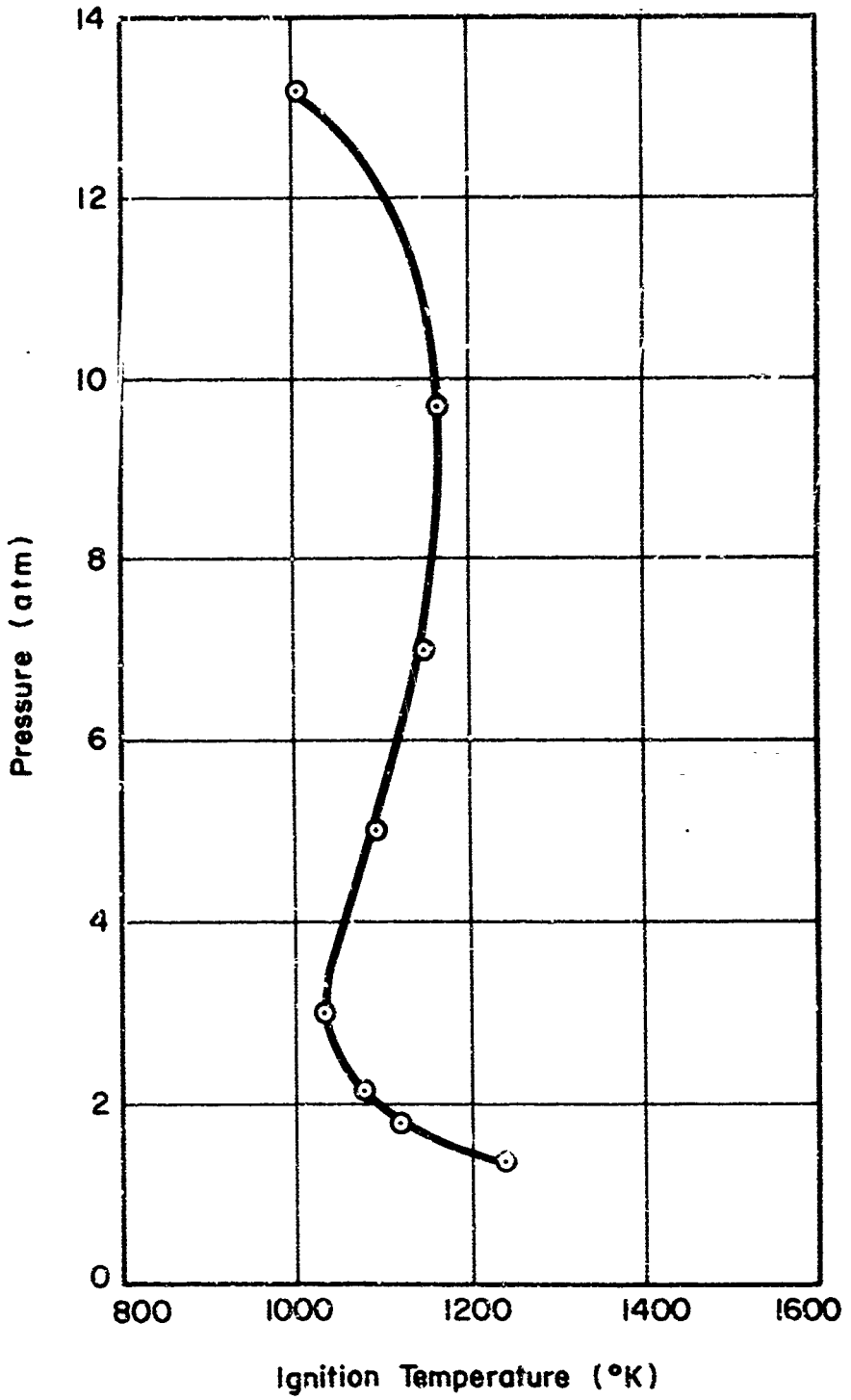

Figure 8 - The Effect of Pressure on the Ignition Temperature of Stoichiometric Methane-Air Mixture (Reflected Shock Data)

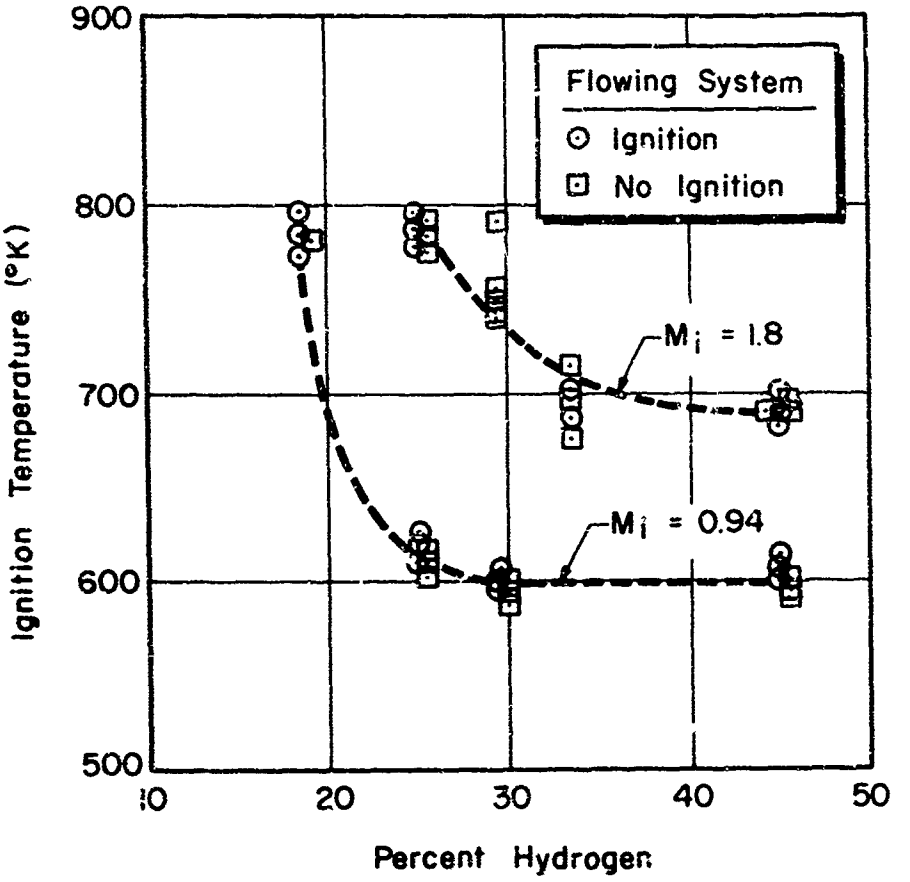

Figure 9 - Shock Ignition Temperatures of Hydrogen-Air Mixtures as a Function of Initial Flow Mach Numbers

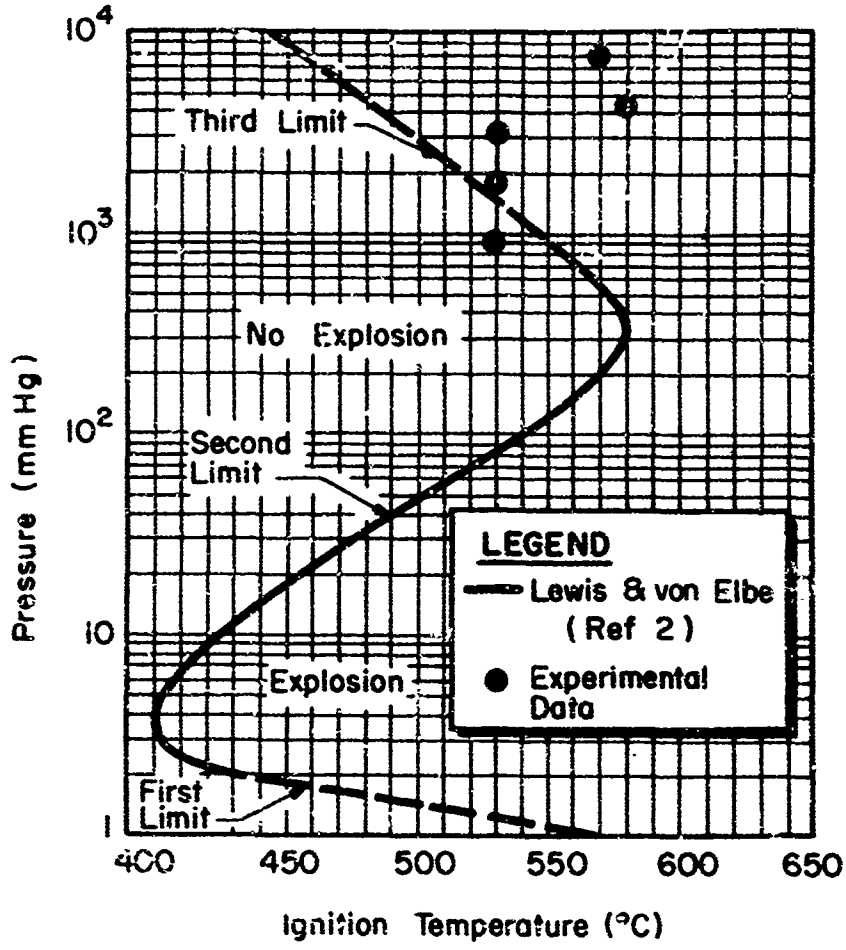

Figure 10 - The Effect of Pressure on the Ignition Temperature of Stoichiometric Hydrogen-Air Mixtures (Reflected Shock Data)

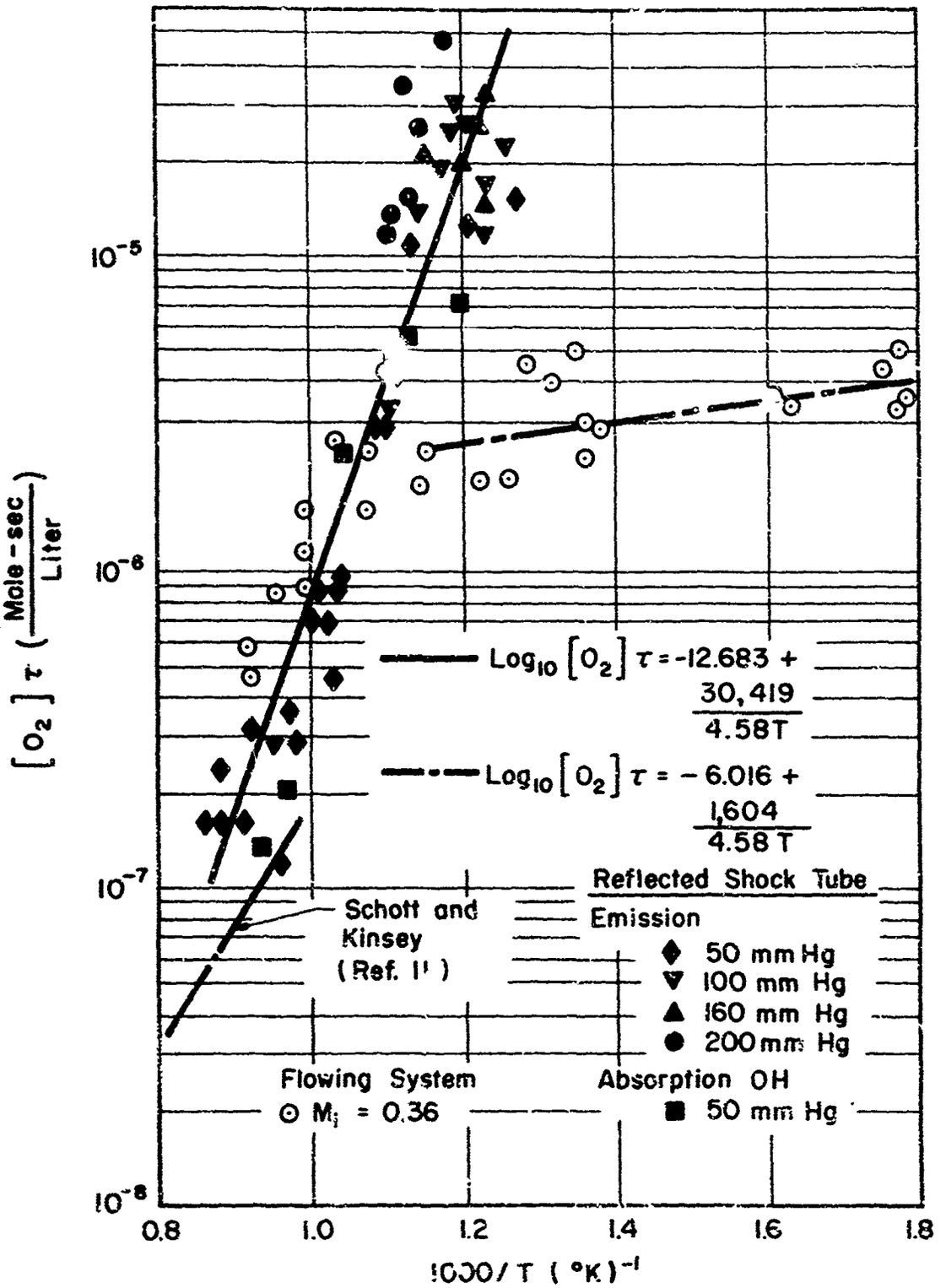

Figure 11 - Ignition Delay Times of Hydrogen-Air Mixtures

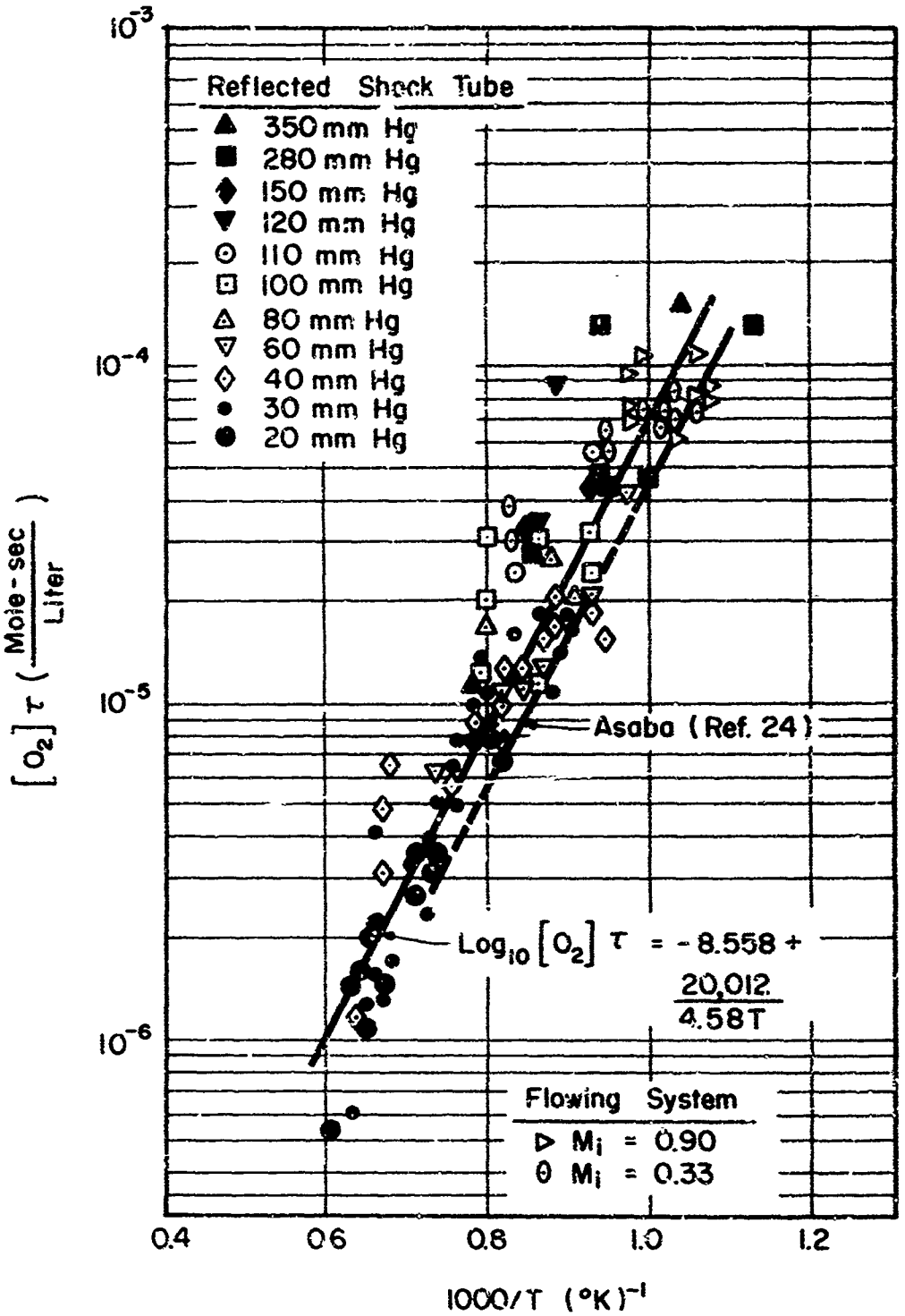

Figure 12 - Ignition Delay Times of Methane-Air Mixtures

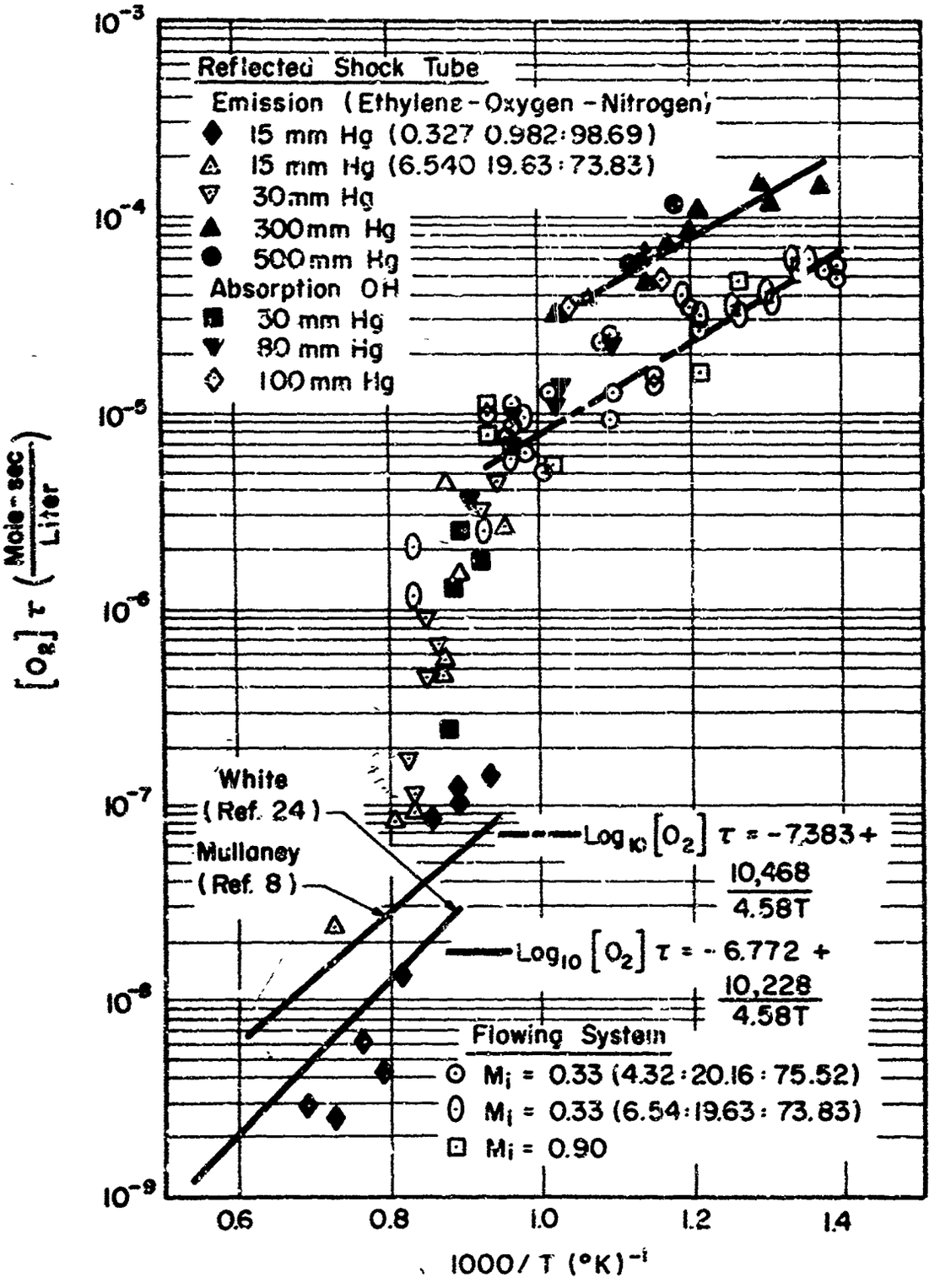

Figure 13 - Ignition Delay Times of Ethylene-Air Mixtures

Table IV - Ignition Delay Times of Stoichiometric Hydrogen-Air Mixtures (Flow System Data)

$\dot{m}_{air}$ = 184 gm/sec η_{air} = 0.704 T_{io} = 278°K
$\dot{m}_{H_2}$ = 5.42 gm/sec η_{H_2} = 0.296 $T_{i,in}$ = 272°K
$M_{i,in}$ = 0.325 $P_{i,in}$ = 1.062 atm $T_{i,x}$ = 271°K
$M_{i,x}$ = 0.36 $P_{i,x}$ = 0.997 atm

T_2(°K)	P_2(atm)	$[O_2]$ (mol/ℓ)	τ (μsec)	$[O_2]\tau \times 10^6$ (mol μsec/ℓ)	$1000/T_2$ (°K^{-1})
759	11.00	0.0262	153.0	4.00	1.317
778	11.45	0.0267	170.1	4.52	1.285
897	14.10	0.0284	84.1	2.38	1.150
930	14.75	0.0287	54.4	1.56	1.075
930	14.75	0.0287	85.5	2.45	1.075
742	10.65	0.0259	192.5	4.98	1.348
724	10.22	0.0254	108.3	2.75	1.382
1051	17.45	0.0300	28.6	0.858	0.952
564	6.74	0.0216	153.0	3.30	1.773
564	6.74	0.0216	236.0	5.09	1.773
571	6.91	0.0220	201.0	4.42	1.750
564	6.74	0.0216	153.0	3.30	1.773
547	6.41	0.0212	175.5	3.73	1.828
972	15.08	0.0286	91.0	2.60	1.03
910	13.77	0.0273	159.0	4.35	1.10
622	7.63	0.0222	166.0	3.68	1.61
735	10.01	0.0244	94.0	2.78	1.36
735	10.01	0.0244	121.0	2.96	1.36
612	7.39	0.0217	157.0	3.4	1.63
1010	15.86	0.0282	31.8	0.898	0.99
1010	15.86	0.0282	55.5	1.56	0.99*
1010	15.86	0.0282	39.7	1.115	0.99
1090	16.26	0.0287	16.3	0.467	0.918
1090	20.76	0.0287	20.8	0.598	0.918*
816	11.53	0.0254	70.9	1.8	1.225
877	12.81	0.0265	40.8	1.85	1.14
795	11.09	0.0251	76.9	1.97	1.26

*Data obtained at second ionization probe detecting ignition.

Table IV - (Continued)
Ignition Delay Times of Stoichiometric Hydrogen-Air Mixtures
(Conventional Shock Tube Data, T_1 = 300°K)

P_1 (mm Hg)	T_r (°K)	P_r (atm)	$[O_2]$ (mol/ℓ)	τ (μsec)	$[O_2]\tau \times 10^6$ (mol μsec/ℓ)	$1000/T_r$ ($°K^{-1}$)
50	1135	2.50	0.00398	40	0.159	0.882
50	988	1.86	0.00341	260	0.867	1.013
50	1107	2.38	0.00389	42	0.163	0.904
50	1007	1.97	0.00345	310	1.07	0.993
50	967	1.81	0.00338	260	0.879	1.035
50	1030	2.06	0.00362	100	0.362	0.972
50	1135	2.51	0.00398	60	0.239	0.882
50	1158	2.60	0.00406	40	0.162	0.863
50	965	1.81	0.00338	140	0.473	1.035
50	920	1.60	0.00316	920	2.91	1.096
50	955	1.76	0.00332	280	0.930	1.047
50	980	1.86	0.00343	200	0.686	1.021
50	994	1.92	0.00349	200	0.715	1.006
50	1082	2.28	0.00279	80	0.303	0.924
50	1046	2.14	0.00370	32	0.118	0.956
50	997	1.93	0.00349	80	0.279	1.005
50	905	1.58	0.00317	1300	4.12	1.110
50	1015	2.01	0.00357	80	0.286	0.985
50	905	1.58	0.00314	920	2.89	1.103
50	885	1.51	0.00308	3540	10.9	1.130
50	825	1.28	0.00280	4470	12.5	1.210
50	785	1.15	0.00264	5840	15.4	1.270
140	1015	5.63	0.00560	50	0.28	0.985
80	1055	3.47	0.00592	50	0.296	0.950
120	840	3.20	0.00688	4740	32.6	1.190
120	855	3.34	0.00705	2950	20.8	1.170
100	810	2.46	0.00548	3100	17.0	1.230
160	825	4.07	0.00889	2980	26.5	1.210
160	815	4.00	0.00885	3840	34.0	1.230
160	870	2.89	0.00596	3860	23.0	1.150
160	830	2.58	0.00561	3600	20.2	1.205
100	878	2.97	0.00613	2300	14.1	1.140
100	812	2.48	0.00551	2160	11.9	1.230
100	847	2.73	0.00589	4310	25.4	1.180
100	830	2.60	0.00563	4580	25.8	1.205
100	790	2.34	0.00524	4360	23.3	1.267
100	765	2.39	0.00562	8340	46.9	1.305
200	913	6.43	0.0127	1000	12.7	1.905
200	875	5.87	0.0120	2200	26.5	1.140
200	895	6.17	0.0125	2900	36.2	1.120
170	905	5.36	0.0107	1200	12.8	1.100
350	905	11.05	0.0219	1700	37.2	1.100
376	852	10.40	0.0219	2280	50.0	1.172
50	885	1.50	0.00306	1805	5.52	1.130
50	900	1.56	0.00317	1550	4.92	1.110
50	965	1.82	0.00338	745	2.52	1.030
50	1070	2.24	0.00377	35	0.132	0.935
50	1003	1.96	0.00347	331	1.15	0.997
50	1035	2.07	0.00364	55	0.200	0.967
50	835	1.32	0.00265	2490	7.1	1.2

Table V - Ignition Delay Times of Methane-Air Mixtures
(Flow System Data)

$\dot{m}_{air}$ = 558.4 gm/sec $\quad \eta_{air}$ = 0.905 $\quad T_{io}$ = 278°K

$\dot{m}_{CH_2}$ = 32.4[illegible] gm/sec $\quad \eta_{CH_4}$ = 0.095 $\quad T_{i,in}$ = 260°K

$M_{i,in}$ = 0.62 $\quad P_{i,in}$ = 1.592 atm $\quad T_{i,x}$ = 243°K

$M_{i,x}$ = 0.90 $\quad P_{i,x}$ = 1.056 atm

T_2(°K)	P_2(atm)	$[O_2]$ (mol/ℓ)	τ (μsec)	$[O_2]\tau \times 10^5$ (mol μsec/ℓ)	$1000/T_2$ (°K^{-1})
923.8	19.9	0.0497	1598	7.95	1.083
923.8	19.9	0.0497	1715	8.53	1.083*
946.4	20.6	0.0509	1578	8.00	1.057
946.4	20.6	0.0509	2090	10.60	1.057*
1020.0	22.8	0.0520	1340	6.95	0.980
1020.0	22.8	0.0520	1425	7.40	0.980*
1025.0	23.1	0.0523	1430	7.48	0.976
1025.0	23.1	0.0523	1970	10.40	0.976*
1028.0	19.85	0.0473	1970	9.35	0.973

$\dot{m}_{air}$ = 178.22 gm/sec $\quad \eta_{air}$ = 0.905 $\quad T_{io}$ = 278°K

$\dot{m}_{CH_4}$ = 10.36 gm/sec $\quad \eta_{CH_4}$ = 0.095 $\quad T_{i,in}$ = 273°K

$M_{i,in}$ = 0.31 $\quad P_{i,in}$ = 1.028 atm $\quad T_{i,x}$ = 272°K

$M_{i,x}$ = 0.33 $\quad P_{i,x}$ = 0.979 atm

T_2(°K)	P_2(atm)	$[O_2]$ (mol/ℓ)	τ (μsec)	$[O_2]\tau \times 10^5$ (mol μsec/ℓ)	$1000/T_2$ (°K^{-1})
967.0	16.8	0.0403	1559	6.03	1.035
1206.0	23.6	0.0448	637	2.85	0.829
1206.0	23.6	0.0448	834	3.72	0.829*
1045.0	18.95	0.0458	1200	5.50	0.947
1045.0	18.95	0.0458	1385	6.33	0.947*
967.0	16.8	0.0403	1559	6.03	1.035
967.0	16.8	0.0403	2049	8.25	1.035
943.0	16.1	0.0394	1844	7.28	1.060
943.0	16.1	0.0394	1712	6.80	1.060*
982.0	17.2	0.0327	1660	6.73	1.020
982.0	17.2	0.0327	1750	7.10	1.020*

*Data obtained at second ionization probe detecting ignition.

Table V (Continued)

(Conventional Shock Tube Data)
Emission Data: Methane-Oxygen-Nitrogen (9.51:19.0:71.49)

P_1 (mm Hg)	T_r (°K)	P_r (atm)	$[O_2]$ (mol/ℓ)	τ (μsec)	$[C_2]\tau \times 10^8$ (mol μsec/ℓ)	$1000/T_r$ ($°K^{-1}$)
20	1570	2.32	0.00343	466	1.595	0.637
20	1525	2.21	0.00332	617	2.05	0.656
20	1540	2.24	0.00337	306	1.03	0.649
20	1410	1.92	0.00316	536	2.64	0.709
20	1570	2.32	0.00343	425	1.435	0.637
20	1370	1.78	0.00302	1108	3.34	0.729
20	1410	1.92	0.00314	1145	3.58	0.709
20	1650	2.61	0.00366	145	0.53	0.606
20	1520	1.91	0.00292	520	1.52	0.658
20	1490	2.11	0.00328	435	1.43	0.672
20	1520	1.92	0.00306	725	2.22	0.658
20	1360	1.76	0.00300	1170	3.5	0.735
20	1375	1.80	0.00304	1130	3.44	0.727
20	1250	1.50	0.00280	2750	7.68	0.800
20	1230	1.47	0.00276	2370	6.55	0.813
20	1570	2.32	0.00344	480	16.5	0.637
280	1065	15.1	0.0329	4000	131.7	0.939
280	1060	15.1	0.0331	1430	47.3	0.944
280	1000	13.4	0.0311	1490	46.4	1.000
350	960	15.2	0.0368	4080	150.0	1.042
280	1055	14.7	0.0323	1630	426.0	0.949
60	1360	5.30	0.00914	690	6.3	0.735
50	1230	3.60	0.0088	1580	10.7	0.814
60	1185	4.06	0.00795	1370	10.9	0.843
60	1155	3.80	0.00762	1654	12.6	0.866
60	1120	3.55	0.00735	2640	19.4	0.893
60	1115	3.32	0.00719	2930	21.0	0.930
60	1040	3.08	0.00688	3100	21.3	0.960
60	1030	3.00	0.00616	6000	40.6	0.971
80	1145	4.88	0.0099	2800	27.7	0.873
80	1100	4.46	0.0094	2130	20.0	0.908
90	1080	4.85	0.0104	3000	31.2	0.926
95	1180	6.18	0.0121	1950	23.6	0.925
98	1265	7.41	0.0136	900	12.25	0.79
98	1188	6.45	0.0126	2360	29.7	0.842
100	1160	6.25	0.0125	2450	30.6	0.862
115	1155	7.13	0.0143	850	12.1	0.865
120	1180	8.50	0.0167	1700	28.4	0.847
120	1130	7.72	0.0158	6200	98.0	0.884
120	1160	8.15	0.0163	1900	31.0	0.862

Table V - (Continued)

P_1 (mm Hg)	T_r(°K)	P_r(atm)	$[O_2]$ (mol/ℓ)	τ (μsec)	$[O_2]\tau \times 10^6$ (mol μsec/ℓ)	$1000/T_r$ ($°K^{-1}$)
40	1350	3.40	0.00585	400	2.34	0.74
45	1225	3.16	0.00598	820	4.92	0.816
45	1216	3.14	0.0060	2780	16.6	0.823
48	1125	2.89	0.00595	3090	18.4	0.889
110	1225	7.74	0.0146	2170	31.7	0.825
110	1205	7.50	0.0144	1700	24.5	0.829
112	1080	5.91	0.0127	4330	55.0	0.926
272	875	9.10	0.0241	5200	126.0	1.14
30	1460	3.04	0.00484	350	1.69	0.684
30	1535	3.40	0.00514	250	1.28	0.651
30	1570	3.47	0.00513	115	0.59	0.637
30	1500	3.20	0.00495	270	1.34	0.667
30	1385	2.72	0.00456	530	2.41	0.722
30	1340	2.57	0.00445	1430	6.35	0.746
30	1250	2.25	0.00418	1985	8.3	0.800
30	1360	2.63	0.00449	1130	5.08	0.735
30	1280	2.37	0.00431	1760	7.6	0.782
30	1260	2.29	0.00423	3290	13.9	0.793
30	1255	2.27	0.0042	1950	8.19	0.796
30	1310	2.45	0.00434	1770	7.69	0.763
30	1260	2.29	0.00423	2500	10.6	0.793
30	1250	2.23	0.00418	2400	10.1	0.800
30	1375	2.70	0.00456	830	3.78	0.727
30	1510	3.24	0.00497	680	4.37	0.662
30	1420	2.86	0.00468	740	3.47	0.704
30	1210	2.07	0.00398	4000	15.9	0.827
30	1275	2.29	0.00417	2360	9.85	0.784
30	1275	2.29	0.00417	2600	10.8	0.784
30	1115	1.8	0.00375	4950	18.5	0.898
30	1155	1.92	0.00386	4760	18.3	0.865
30	1105	1.76	0.00370	4550	16.6	0.905
30	1125	1.82	0.00374	3750	14.0	0.89
30	1130	1.84	0.00378	2760	10.4	0.885
40	1153	2.55	0.00514	2970	15.3	0.867
40	1125	2.42	0.00499	3550	17.7	0.888
40	1130	2.45	0.00503	4150	20.9	0.885
40	1060	2.13	0.00466	3330	15.50	0.944
40	1080	2.21	0.00473	3940	18.6	0.926
40	1532	4.40	0.00670	180	1.2	0.653
40	1490	4.20	0.00652	475	3.1	0.671
40	1325	3.37	0.00590	970	5.72	0.755
40	1490	4.21	0.00656	745	4.9	0.671
40	1455	4.00	0.00637	1050	6.7	0.687
40	1275	3.10	0.00565	1560	8.8	0.784

Table V - (Continued)

P_i (mm Hg)	T_r (°K)	P_r (atm)	$[O_2]$ (mol/ℓ)	τ (μsec)	$[O_2]\tau \times 10^6$ (mol μsec/ℓ)	$1000/T_r$ ($°K^{-1}$)
40	1270	3.10	0.00565	1650	9.34	0.787
40	1236	2.92	0.00548	1790	9.8	0.810
40	1220	2.87	0.00545	2280	12.4	0.820
40	1190	2.71	0.00528	2370	12.5	0.840
100	1250	7.50	0.0139	2200	30.6	0.80
100	1255	7.57	0.0139	1390	19.4	0.795
110	1195	7.53	0.0146	2070	30.2	0.837
150	1228	10.85	0.0205	380	7.8	0.814
155	1180	10.30	0.0203	1670	33.8	0.847
200	1067	11.05	0.0240	1930	46.4	0.938
75	1250	5.63	0.0104	1590	16.6	0.800
30	1310	2.49	0.00441	1120	4.94	0.764

Table VI - Ignition Delay Times of Ethylene-Air Mixtures
(Flow System Data)

$\dot{m}_{air}$ = 184.4 gm/sec $\quad \eta_{air}$ = 0.9346 $\quad T_{io}$ = 283°K

$\dot{m}_{C_2H_4}$ = 12.5 gm/sec $\quad \eta_{C_2H_4}$ = 0.0654 $\quad T_{i,in}$ = 278°K

$M_{i,in}$ = 0.31 $\quad P_{i,in}$ = 1.054 atm $\quad T_{i,x}$ = 277°K

$M_{i,x}$ = 0.33 $\quad P_{i,x}$ = 1.003 atm

T_2(°K)	P_2(atm)	$[O_2]$ (mol/ℓ)	τ (μsec)	$[O_2]\tau \times 10^6$ (mol μsec/ℓ)	$1000/T_2$ (°K^{-1})
747.0	11.65	0.0372	1392	51.60	1.340
1039.5	18.65	0.0428	137	5.86	0.967
844.0	13.95	0.0394	995	39.20	1.185
844.0	13.95	0.0394	1037	40.80	1.185*
747.0	11.65	0.0372	1430	53.20	1.340
747.0	11.65	0.0372	1546	57.70	1.340*
767.0	12.10	0.0375	1021	38.40	1.305
767.0	12.10	0.0375	1060	39.60	1.305*
825.0	13.53	0.0392	757	29.60	1.212*
825.0	13.53	0.0392	778	30.50	1.212
803.0	12.93	0.0386	807	31.00	1.255
803.0	12.93	0.0386	807	31.00	1.255*
1200.7	22.55	0.0447	48.1	2.10	0.833
1200.7	22.55	0.0447	28.9	1.29	0.833
1039.5	18.65	0.0426	191.7	8.18	0.962
1078.4	19.61	0.0435	55.6	2.42	0.928

$\dot{m}_{air}$ = 565.13 gm/sec $\quad \eta_{air}$ = 0.9346 $\quad T_{io}$ = 278°K

$m_{C_2H_4}$ = 38.3 gm/sec $\quad \eta_{C_2H_4}$ = 0.0654 $\quad T_{i,in}$ = 260°K

$M_{i,in}$ = 0.62 $\quad P_{i,in}$ = 1.627 atm $\quad T_{i,x}$ = 244°K

$M_{i,x}$ = 0.90 $\quad P_{i,x}$ = 1.072 atm

1075	24.6	0.0548	184	10.10	0.93
990	22.2	0.0537	97	5.20	1.01
1075	24.6	0.0548	142	7.79	0.93
1172	27.5	0.0561	139	7.8	0.85
829	17.45	0.0502	329	16.50	1.207
795	16.42	0.0494	762	37.60	1.26
826	17.35	0.0499	237	11.85	1.21

Table VI - (Continued)

$\dot{m}_{air}$ = 184.38 gm/sec η_{air} = 0.9568 T_{io} = 283°K

$\dot{m}_{C_2H_4}$ = 8.065 gm/sec $\eta_{C_2H_4}$ = 0.04322 $T_{i,in}$ = 278°K

$M_{i,in}$ = 0.31 $P_{i,in}$ = 1.054 atm $T_{i,x}$ = 277°K

$M_{i,x}$ = 0.33 $P_{i,x}$ = 1.000 atm

T_2(°K)	P_2(atm)	$[O_2]$ (mol/ℓ)	τ (μsec)	$[O_2]\tau \times 10^6$ (mol μsec/ℓ)	$1000/T_2$ (°K^{-1})
1042.5	18.70	0.044	274	12.10	0.959
1042.5	18.70	0.044	165	7.26	0.959
977.2	17.10	0.043	116	4.98	1.023
977.2	17.10	0.043	107	4.60	1.023*
870.1	14.50	0.0409	235	9.61	1.150*
1042.5	18.70	0.044	183	8.06	0.959
1042.5	18.70	0.044	155	6.82	0.959*
920.2	15.75	0.042	319	13.40	1.087
920.2	15.75	0.042	216	9.02	1.087*
870.1	14.50	0.0409	362	14.80	1.150
828.4	13.50	0.040	635	25.40	1.208
920.2	15.75	0.042	648	27.40	1.087
920.2	15.75	0.042	604	25.70	1.087*
720.0	10.90	0.0374	1013	37.70	1.389
720.0	10.90	0.0374	1013	37.70	1.389*
720.0	10.90	0.0374	1097	41.00	1.389
720.0	10.90	0.0374	1223	45.80	1.389

*Data obtained at second ionization probe detecting ignition

Table VI - (Continued)

(Conventional Shock Tube Data)
(Emission Data: Ethylene-Oxygen-Nitrogen (6.54:19.63:73.83)

P_i (mm Hg)	T_r (°K)	P_r (atm)	$[O_2]$ (mol/ℓ)	τ (μsec)	$[O_2]\tau \times 10^6$ (mol μsec/ℓ)	$1000/T_r$ ($°K^{-1}$)
204	1140	12.75	0.0267	170	4.54	0.876
300	982	13.50	0.0328	920	30.2	1.018
295	942	12.07	0.0306	1210	37.0	1.062
296	876	10.28	0.02805	1550	43.5	1.141
296	857	9.74	0.02715	2600	70.55	1.168
300	830	9.08	0.0262	3200	83.7	1.204
296	827	8.88	0.02565	4000	102.6	1.21
300	773	7.70	0.0238	6430	153.0	1.294
298	767	7.49	0.02333	5230	124.0	1.306
300	732	6.71	0.0220	6870	151.0	1.369
525	850	16.9	0.046	2790	128.0	1.18
475	893	17.2	0.0447	1300	58.2	1.12
15	1250	1.132	0.00216	40	0.0864	0.8
15	1145	0.942	0.00195	240	0.47	0.873
15	1153	0.865	0.00194	270	0.523	0.865
15	1120	0.903	0.00192	730	1.4	0.892
15	1058	0.800	0.00179	1430	2.56	0.945
15	965	0.652	0.00160	2280	3.65	1.036
15	1035	1.062	0.00210	45	0.0945	0.826
15	1150	1.40	0.00199	12	0.0234	0.716
30	1210	2.12	0.00418	25	0.1045	0.829
30	1175	1.99	0.00404	220	0.89	0.852
30	1215	2.14	0.0042	40	0.168	0.823
30	1175	1.99	0.00404	190	0.44	0.852
30	1085	1.68	0.00369	830	3.06	0.922
30	1155	1.92	0.00296	160	0.632	0.865
30	1066	1.62	0.00364	1150	4.18	0.938
30	915	1.15	0.00303	7350	22.2	1.09
30	980	1.34	0.00320	3260	10.4	1.02
30	990	1.38	0.00334	3870	12.9	1.01
Absorption-OH						
30	1120	1.81	0.00383	650	2.5	0.893
30	1042	1.54	0.00354	1940	6.85	0.960
30	990	1.86	0.00392	350	1.37	0.881
30	1087	1.69	0.00370	450	1.67	0.920
30	1140	1.87	0.00392	60	0.236	0.877
100	965	4.35	0.0108	3300	35.6	1.037
100	865	3.34	0.00925	4900	45.2	1.16
80	1035	4.05	0.00935	950	8.9	0.965
70	1100	4.02	0.00875	360	3.16	0.910

Table VI - (Continued)

P_1 (mm Hg)	T_r(°K)	P_r(atm)	$[O_2]$ (mol/ℓ)	τ (μsec)	$[O_2]\tau \times 10^6$ (mol μsec/ℓ)	$1000/T_r$ ($°K^{-1}$)
Reflected Shock	Ethylene-Oxygen-Nitrogen (0.327:0.982:98.691)					
15	1333	1.05	0.0000954	20	0.19	0.752
15	1450	1.24	0.0001025	30	0.3074	0.690
15	1312	1.02	0.0000850	65	0.608	0.762
15	1270	0.958	0.000090	90	0.436	0.789
15	1320	0.905	0.000068	155	1.39	0.813
15	1120	0.750	0.0000805	1470	11.8	0.894
15	1115	0.746	0.000080	1330	10.7	0.897
15	1080	0.700	0.000078	1900	14.7	0.926
15	1175	0.830	0.000085	1000	8.5	0.852

P_1(mm Hg)	T_2(°K)	P_2(atm)	$[O_2]$ (mol/ℓ)	τ (μsec)	$[O_2]\tau \times 10^6$ (mol μsec/ℓ)	$1000/T_2$ ($°K^{-1}$)
Incident Shock	Ethylene-Oxygen-Nitrogen (0.20:4.0:95.8) (mixture studied by White)					
15	1205	0.394	0.000158	750.0	11.8	0.829
15	1355	0.460	0.000166	468.0	7.76	0.737
15	1420	0.500	0.000171	760.0	13.0	0.704
15	1520	0.570	0.000177	27.6	0.488	0.658
15	1500	0.550	0.000172	22.0	0.278	0.667
15	1170	0.375	0.000156	681.0	10.6	0.855

did not produce autoignition. When the basic configuration apparatus was used (Fig. 3a) and when the oxidizer flow rate was greater than 400 g/sec, autoignition of the mixture occurred as soon as hydrogen was admitted. On the other hand when the fuel and oxidizer flows were started simultaneously, autoignition occurred at approximately the same oxidizer flow rate but only after a time delay. It cannot be stated with certainty that oxygen flow rates of less than 400 g/sec would not lead to autoignition. However, for mixing tubes shorter than 6.3 cm, autoignition never occurred. In another apparatus having the same mixing tube diameter, the fuel and the oxidizer flows entered as parallel jets which were produced by placing a partition into the lower section of the tube. Although various flow speeds and mixture ratios were employed, autoignition never occurred in this apparatus. However, when a small flat plate was placed one inch from the tube exit normal to the flow, ignition occurred quite readily. It should be remembered that the above autoignition data were taken with the apparatus shown in Fig. 3. Other geometries and other scales could produce different results. On the whole it was not possible to establish the precise conditions leading to autoignition because of the complex nature of the phenomenon.

Possible ionization of the fuel or oxidizer gas flow was investigated; however, no significant ionization was detected for the flow rates of oxygen or air employed in the previous experiments.

Since the basi tube geometry shown in Fig. 3a readily produced autoignition of the hydrogen-oxygen mixtures, hydrogen-air mixtures were also tested in this apparatus. However, no autoignition of this mixture occurred even at mass flow rates of 500 g/sec air and 30 g/sec hydrogen. These flow rates are higher than those required to produce spontaneous ignition in hydrogen-oxygen mixtures.

With the basic tube configuration shown in Fig. 3a, measurements of the temperature and the pressure at various positions along the mixing tube and inlet tube lines were made. This study revealed that at certain oxidizer flow rates (without fuel addition) significant temperature and pressure fluctuations occur in the fuel line near the mixing chamber. Zones of high temperature occurred at certain distances from the mixing chamber. These hot zones appeared to be produced by a resonance phenomenon in the fuel chamber. A shielded chromel-alumel thermocouple was used to obtain the maximum steady-state temperature. Because of the relatively large thermocouple mass, several minutes were required for the thermocouples to reach temperature equilibrium. The maximum gas temperature measured for a mix line 50 cm long was 770°K, while for a 6.3 cm long tube the maximum temperature measured was 1075°K (radiation losses not accounted for). The stagnation temperature of the oxidizer flow was 290°K. The slow response of the thermocouple did not permit the measurement of any variation of the gas temperature with time.

The pressure variations along the fuel line were also measured. Standing waves of three different frequencies were observed as a function of the oxidizer mass flow rate. Resonant frequencies of 600, 750, and 2000 Hz appeared. The 2000 Hz mode occurred at a flow which corresponded to that at which spontaneous ignition of the hydrogen-oxygen mixture occurred and also which produced the highest gas temperatures in the fuel line. Sound level measurements at the exit of the mixture tube were also taken. At the 3rd mode (2000 Hz), sound pressure levels of 130 dB were measured.

The above measurements were made in a fuel line which was closed upstream. The pressure probe was located at the closed end of the line. To establish whether the same resonance conditions exist with a gas flow in the resonance chamber, the measurements were repeated with various flow rates of air through the fuel line. The resonant frequencies decreased as these flow rates were increased. The 600 and 750 Hz modes were eliminated by moderate amounts of counter flow. Figure 14 shows the decrease of frequency with counter flow for the three modes. The 2000 Hz mode was intermittent for fuel line flow rates above 15 g/sec. Figure 15 shows the average (due to filtering of the electrical signal) wave shape variation caused by various fuel line flow rates.

Streak schlieren photographs and stop action sequential schlieren-photographs were made of the wave pattern in a fuel line consisting of a tube with a 0.95 cm-square cross section and a 10 cm length. Typical photographs of the pressure-time diagrams at the end wall of the tube are given in Figs. 16 and 17, respectively for the second characteristic mode (750 Hz). The third and most severe resonant mode (2000 Hz) could not be excited in this fuel line. However, when the corners of the base of the flow tube were filleted, the third mode appeared. As seen in the stop action photographs (Fig. 16), the second mode is a series of normal shocks moving along the length of the fuel line. Also, a series of complicated wave interactions is generated behind the waves. Each photograph of this figure represents the resonant wave configuration at a given time after the main (leading) normal shock has reflected off the back wall of the fuel line chamber. Since the experimental set-up was such that only a single photograph was possible during each experiment, each photograph represents a different cycle. Therefore, the waves and wave interactions vary from one photograph to another. Continuous variations of the wave forms from cycle to cycle are visible in the pressure traces and streak schlieren photographs (Fig. 17).

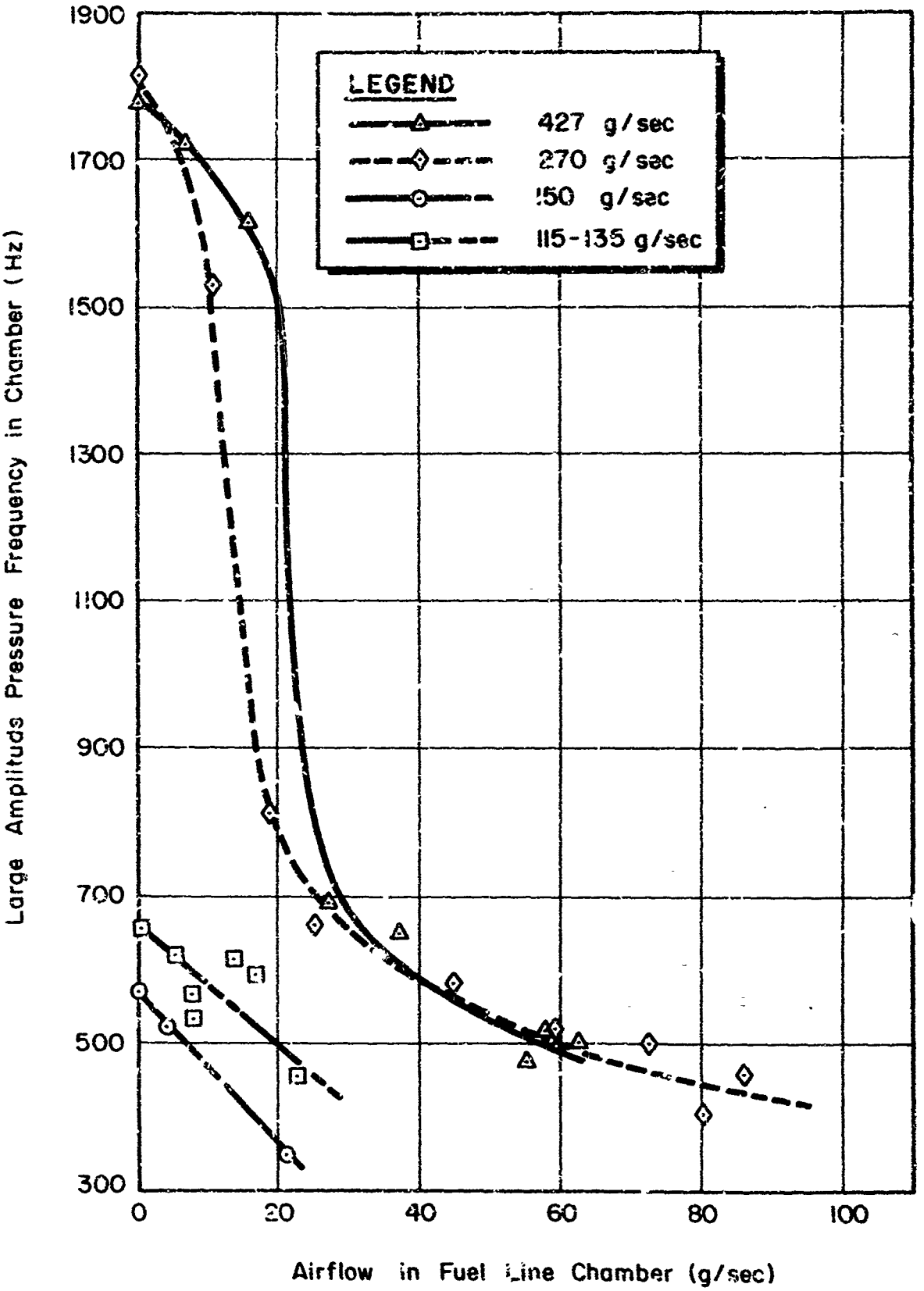

Figure 14 - The Variation of Pressure Fluctuations as a Function of Fuel Line Mass Flow Rate

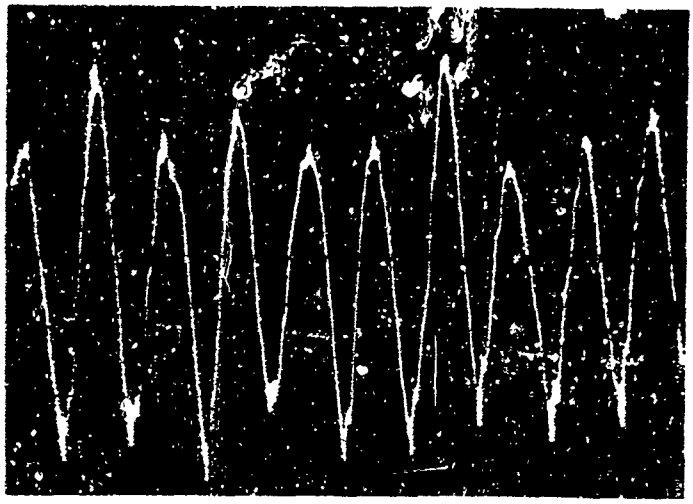

$\dot{m}_p$ = 270 g/sec
$\dot{m}_{RC}$ = 0.0 g/sec
F_{RC} = 1916 Hz

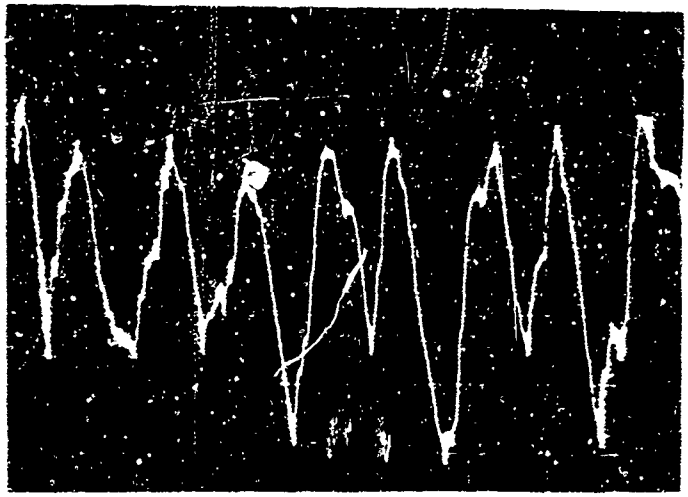

$\dot{m}_p$ = 270 g/sec
$\dot{m}_{RC}$ = 10.5 g/sec
F_{RC} = 1629 Hz

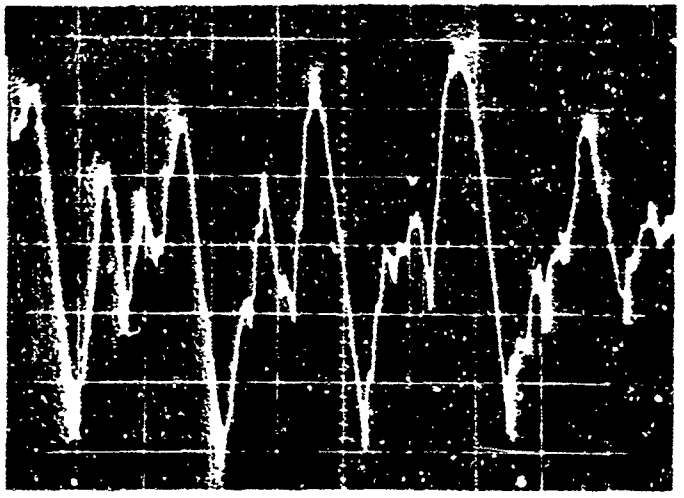

$\dot{m}_p$ = 270 g/sec
$\dot{m}_{RC}$ = 18.9 g/sec
F_{RC} = 910 Hz

Time (500 μsec/div)

Figure 15a - Oscillograph Traces of Pressure Variations in Fuel Line as a Function of Mass Flow Rate through Fuel Line

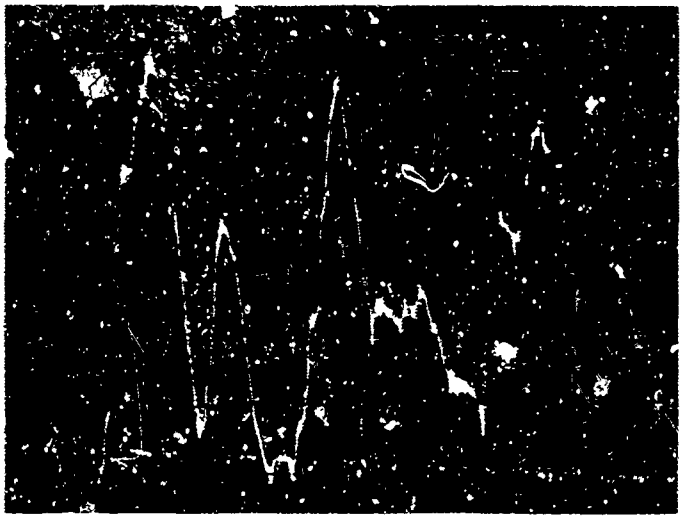

$\dot{m}_p$ = 270 g/sec
$\dot{m}_{RC}$ = 24.8 g/sec
F_{RC} = 760 Hz

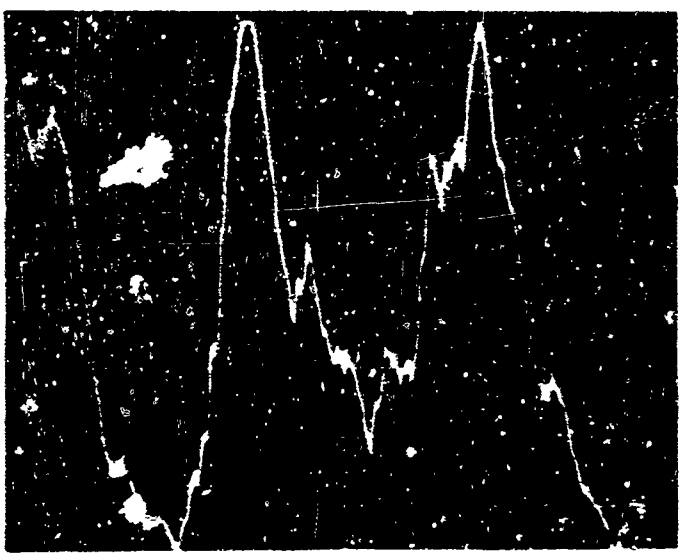

$\dot{m}_p$ = 270 g/sec
$\dot{m}_{RC}$ = 44.2 g/sec
F_{RC} = 615 Hz

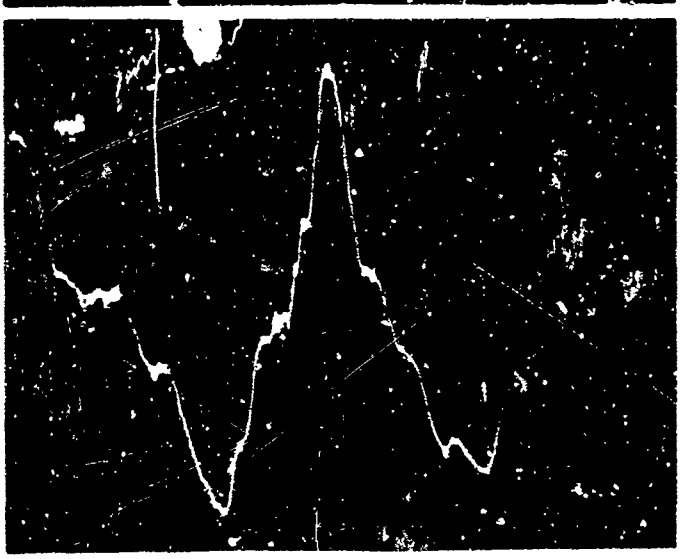

$\dot{m}_p$ = 270 g/sec
$\dot{m}_{RC}$ = 81 g/sec
F_{RC} = 500 Hz

Time (500 μsec/ div)

Figure 15b - Oscillograph Traces of Pressure Variations in Fuel Line as a Function of Mass Flow Rate through Fuel Line

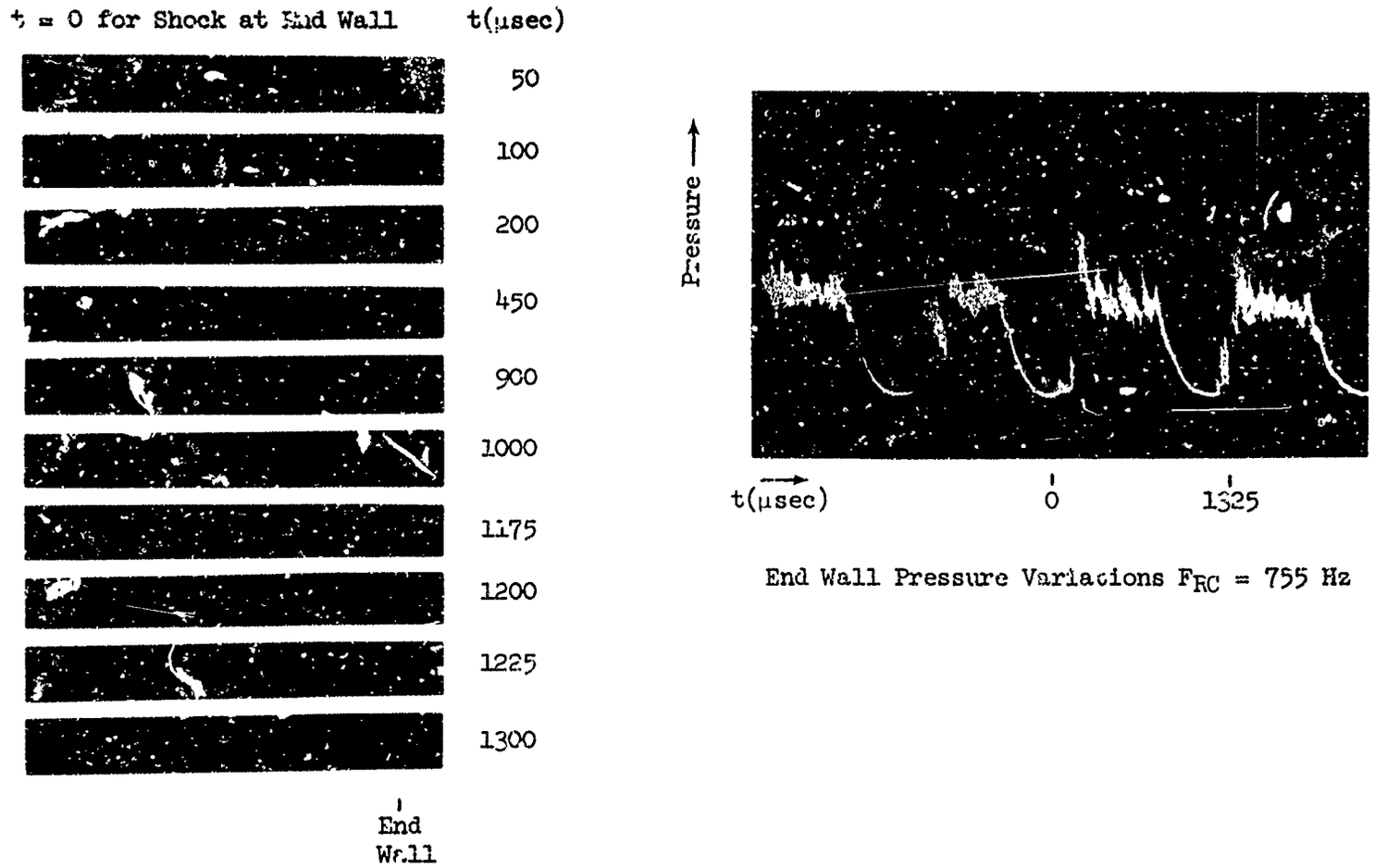

End Wall Pressure Variations F_{RC} = 755 Hz

Figure 16 - Stop Action Schlieren Photographs and End Wall Pressure Variations of a Square Fuel Line

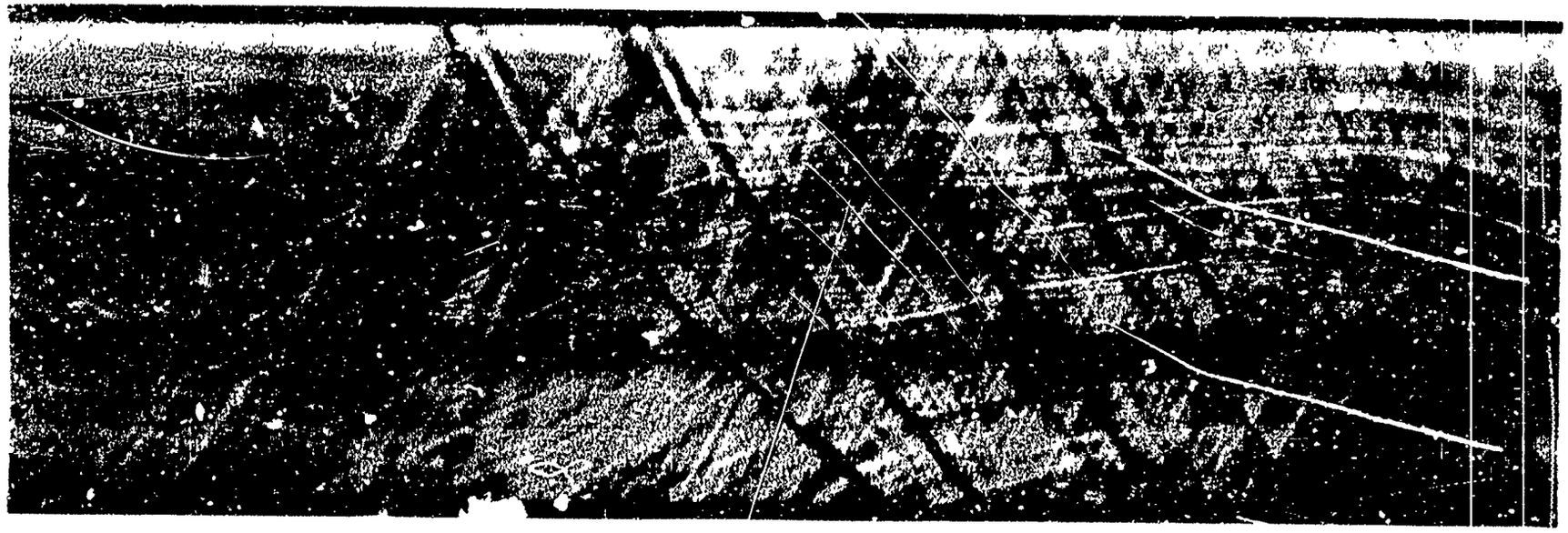

Time Resolution = 50.8 μsec/cm
Magnification = 0.825

Film Speed = 6470 cm/sec
F_{RC} = 750 Hz

$\dot{m}_p$ = 66 g/sec
$\dot{m}_{RC}$ = 0.0 g/sec

Figure 17 - Streak Schlieren Photograph of Pressure Waves in a Square Fuel Line

IV. DISCUSSION OF RESULTS

The observation that flowing fuel-oxidizer mixtures often ignite spontaneously at temperatures (static and total) far below the measured thermal ignition temperatures of static systems[3,6,7] has led to the speculation that the ignition mechanism of flowing mixtures is somewhat different from that of static mixtures. An investigation of the electrical properties of flowing air and flowing oxygen gases did not reveal any significant buildup of electric charges in these gases. Moreover, the ignition delay times observed in flowing mixtures (hydrogen-air, methane-air, and ethylene-air Figs. 11, 12, and 13, respectively) do not vary significantly from those observed for nonflowing mixtures. Therefore, the mechanism of ignition of the mixture is not believed to be altered by the ordered flow velocity. However, the fact that the gas mixture is moving is important to the basic problem because of hydrodynamic phenomena such as stagnation conditions, generation of waves, and wave interactions (resonance). The shock waves were driven into the mixtures in a direction opposite to the mixture velocity. The pertinent ignition test conditions (temperature, pressure, and velocity), therefore, are those which exist behind the shock wave.

The minimum ignition temperatures of flowing hydrogen-air mixtures obtained by this technique (Fig. 2) are presented in Table I. The minimum ignition temperature is a function of the particle Mach number (or particle velocity) and the static pressure of the unburned gas; graphs depicting these relationships are presented in Figs. 18 and 19. The data in these graphs were taken for a variety of hydrogen-air mixture ratios and initial flow Mach numbers. Only the value obtained with a very lean mixture (18 percent hydrogen) deviates significantly from the other measurements.

Pressure is known to have a significant effect on the minimum ignition temperatures of static hydrogen-oxygen-nitrogen mixtures. Lewis and von Elbe[2] reported three explosion limit regions as a function of pressure (shown in Fig. 10). The authors explained these limits on the basis of reaction kinetics and involve the appearance or disappearance of the H and the HO_2 species. The ignition temperatures at various pressures for static hydrogen-air mixtures (measured behind reflected shock waves) are tabulated in Table I and graphically shown in Fig. 10. These values fall into the high-pressure region (third explosion limit) and they agree quite well with the reflected shock tube data of Steinberg and Kaskan[20] for hydrogen-oxygen mixtures and with the values published by Craig[7] for hydrogen-air mixtures. The test times of the present shock tube apparatus was limited to 7000 μsec. If longer test times had been available, then it may have been possible that lower minimum ignition temperature values could have been determined since the ignition delay times are longer for lower temperatures. Although the observed ignition temperatures are nearly the same as those reported by Lewis and von Elbe, they do not exhibit the predicted

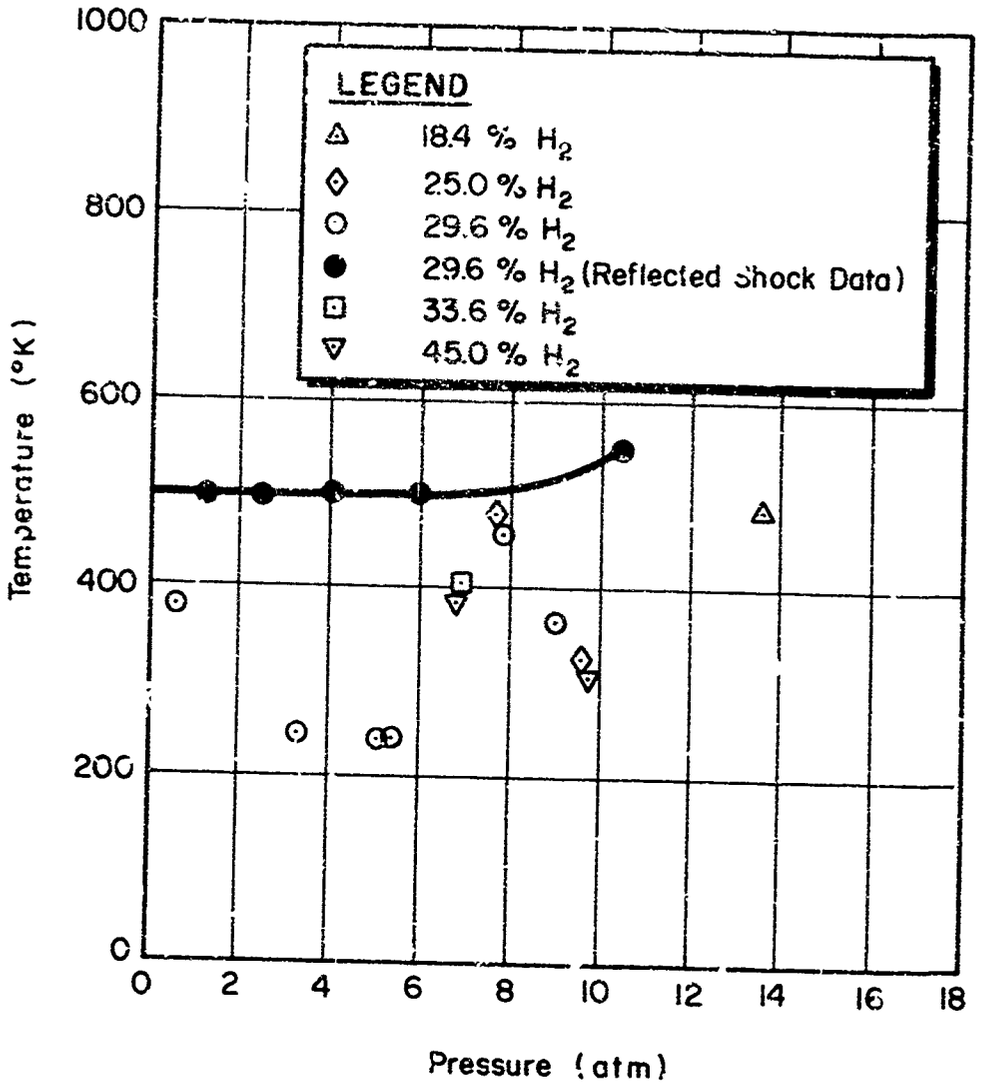

Figure 18 - The Effect of Pressure on the Ignition Temperature of Flowing and Static Hydrogen-Air Mixtures

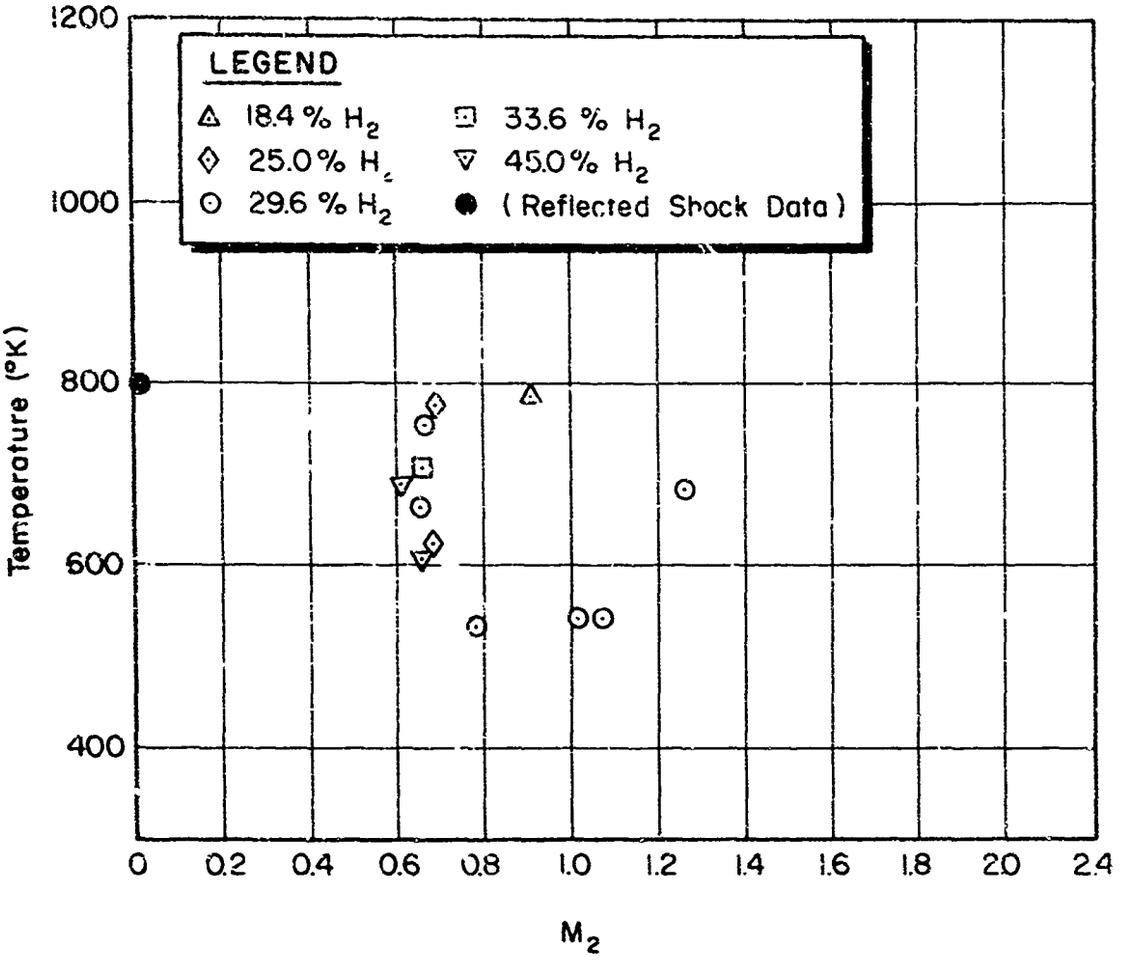

Figure 19 - Ignition Temperature Versus Particle Mach Number for Hydrogen-Air Mixtures

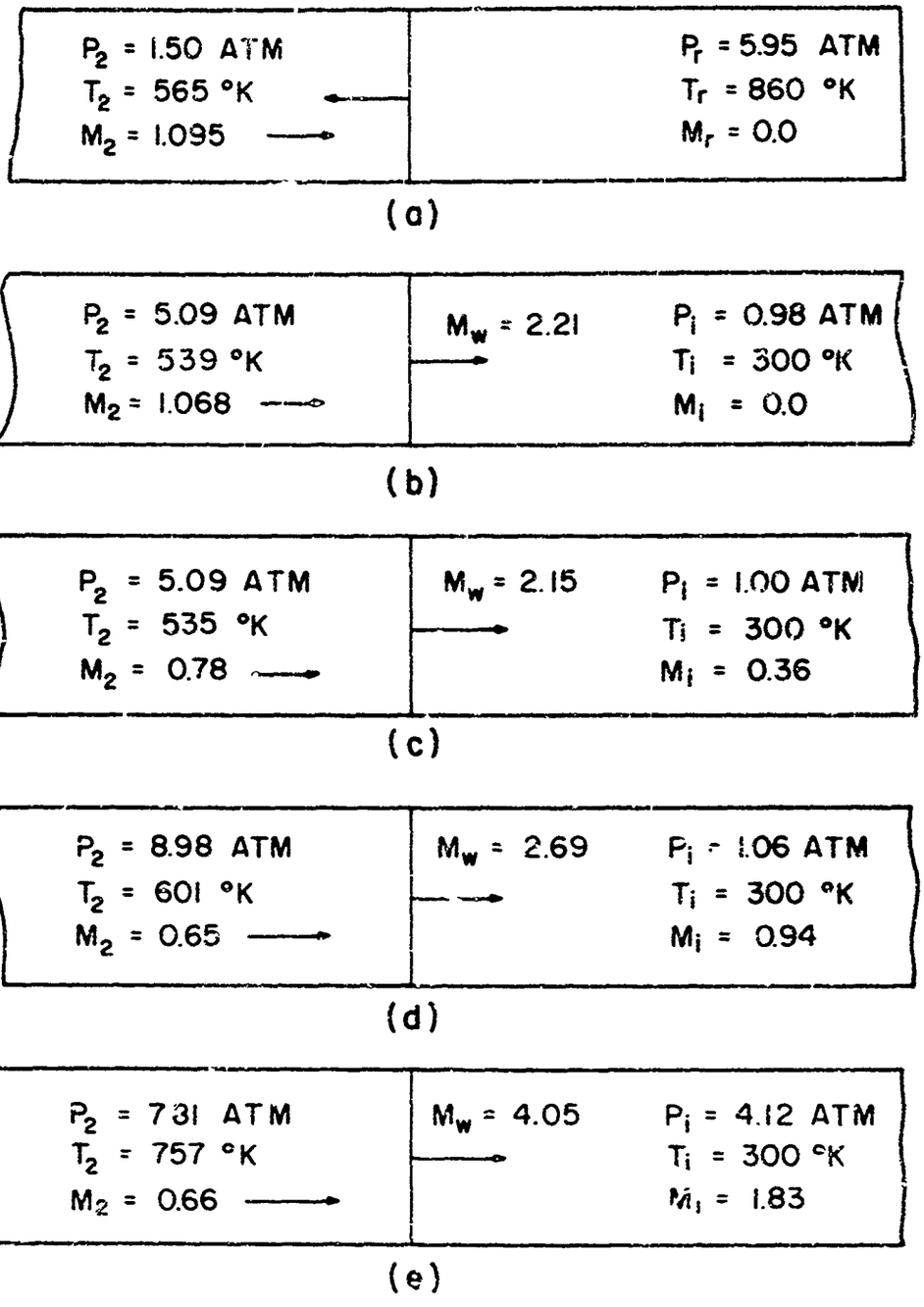

Figur 20 - Conditions Illustrating the Effect of Gas Flow on the Ignition Temperature of Stoichiometric Hydrogen-Air Mixtures

trend that the ignition temperatures in the third limit region decrease with increasing pressure.

The minimum ignition temperatures as a function of static pressure for the case of flowing combustible gas mixtures are tabulated in Table I and plotted in Fig. 18. A comparison of these data with those obtained in stationary mixtures (also plotted in the figure) shows that the minimum ignition temperatures are considerably lower when the gases are flowing. This observation agrees with the results obtained by other researchers[3,6,7] who used incident shock waves to measure minimum ignition temperatures. Craig[7] measured ignition temperatures of hydrogen-air mixtures behind both incident and reflected shock waves. For the stoichiometric hydrogen-air mixture, he obtained ignition temperatures of 440 and 880°K behind the incident (flow) and reflected (static) shock waves, respectively. The measurements were made at static pressures of approximately 1 and 2 atm, respectively. Craig explained the discrepancy by assuming that flaking of solid particles (scale) from the tube wall occurred. Belles[3] and Fay[6] attributed the variation to wave interactions behind the incident shock wave.

To examine the effects of the gas flow further, it is worthwhile to compare several of the ignition temperature data points which have similar conditions. In Fig. 20 these data are compiled for a stoichiometric hydrogen-air mixture; Fig. 20a gives the minimum ignition conditions behind a reflected shock wave. The pressure in this case is 5.45 atm, while the ignition temperature is 860°K. Figures 20b-d give the ignition temperatures behind incident shock waves where the static pressure is approximately 7.1 atm. The minimum ignition temperature for these cases is 539, 535, and 601°K for conditions where the particle Mach number is 1.0, 0.75, and 0.65, respectively. The last data point in this series has a higher ignition temperature, which tends to suggest that the ignition is related to the particle Mach number (velocity). For the case shown in Fig. 20c, the minimum ignition temperature was 757°K at a static pressure of 7.8 atm. The particle Mach number for this case was 0.66. When the particle Mach number, pressure, and temperature are slightly below these values, no ignition can be expected. The values of pressure and temperature for ignition of cases shown in Figs. 20b-d are considerably below those of the latter case. These data give further evidence that the particle Mach number has an effect on the ignition of the mixture. No ignitions were observed at temperatures lower than the static ignition temperature when the particle Mach numbers were less than 0.60 (Table I). For the result in Fig. 20a the reflected wave is propagating into a mixture having a static temperature of 540°K, a pressure of 2.7 atm, and a Mach number of 1.095. That this condition did not lead to ignition indicates that the static pressure of the flowing mixture also influences the ignition temperature of the mixture.

A graph showing the ignition temperatures as a function of particle Mach number for all mixtures studied is given in Fig. 19. Only the lean

mixture data points deviated from the overall trend of the data. Generally, the lowest ignition temperatures occur for a Mach number between 0.8 and 1.0. As stated above, Belles[3] suggested that the minimum ignition temperature for flowing gas mixtures is affected by wave interactions. Hydrodynamic resonance generated by a flowing gas has been observed in another phase of the present investigation (to be discussed later). This phenomenon has been found to produce temperatures and pressures which are considerably higher than the initial static values. Powerful acoustic waves due to flow over cavities have been reported by East[21] and Plumbee et al.[22] Shapiro[23] analysed the resonance problem in an approximate manner and concluded that local temperatures in resonance waves can reach values several times the stagnation values.

The minimum ignition temperature values obtained for stoichiometric ethylene-air and methane-air for both flowing and static cases are given in Tables II and III. In both of these systems, the minimum ignition temperatures were found to depend only on the static pressure. The maximum ignition delay times for these systems were found to be 2200 and 3400 μsec. If longer test times had been available, an effect of the particle gas flow might have been detected. The ignition temperatures obtained for these two systems agree with the values obtained in static mixtures by Kane et al.[5] Shepherd[4] measured the ignition temperatures of methane-oxygen and ethylene-oxygen mixtures behind incident shock waves (flowing gases) and reported ignition temperatures several hundred degrees below those observed in stationary mixtures. Assuming that diluents have no effect on the minimum ignition temperatures (as in the hydrogen-oxygen case), then flowing methane-air and flowing ethylene-air mixtures may also be expected to ignite at temperatures lower than those observed for static mixtures. Here again, ignition would probably be caused by higher local temperatures and pressures as a result of wave interaction phenomenan.

The ignition delay times of stoichiometric methane-air, hydrogen-air, and ethylene-air mixtures as a function of temperature are tabulated in Tables IV, V, and VI and graphically shown in Figs. 11, 12, and 13, respectively. Using the method of least mean squares, empirical equations representing the experimental data were obtained. They are given in the figures. As seen from Fig. 12, the ignition delay times for the methane-air mixtures are the same for both the flowing and the static mixtures. These results are in agreement with those observed with lean methane-oxygen mixtures reported by Asaba.[24] The ignition delay times of static hydrogen-air mixtures (Fig. 11) agree generally with the static ignition delays reported by Shott and Kinsey.[11] For flowing mixtures whose temperatures are below the static minimum ignition temperature, the ignition delay times tend to level out. Since it has been established that no significant changes in the electrical properties of the gases occur at the temperatures and flow velocities involved, no changes in the kinetics of the ignition mechanism are believed to occur. Therefore, the lower ignition delay times for these mixtures suggest that the temperatures of these flowing mixtures are (at least

locally) higher than the average values calculated from shock theory. These higher temperatures are probably the result of heating by wave interactions (resonance).

Most of the ignition delay time measurements of ethylene-air mixtures (Fig. 13) have been made at higher pressures and lower temperatures than those generally available in the literature. For the static mixtures at low pressures and high temperatures, the results generally agree with those of Mullany[8] and also with those of White.[25] The ignition delay times for this mixture increase suddenly by a factor of 100 near 1150°K. Apparently a significant change in the overall kinetic mechanism occurs at the higher temperatures. It is noted from Fig. 13 that the ignition delay times in flowing gases are shorter than the corresponding values in static mixtures.

Autoignitions of flowing hydrogen-oxygen mixtures have been found to depend on the mass flows and the geometry of the flow apparatus. For the apparatus shown in Fig. 3a, a minimum mass flow of 400 g/sec was required to produce autoignition in the mixtures. At this mass flow rate, a 2000 Hz resonant frequency (third mode) was excited in the fuel line. This mode was exited only when the fuel and oxidizer lines to the mixing chamber were diametrically opposed. This resonant mode was set up in the hydrogen line whether a hydrogen flow existed or not. When the mixing tube was shortened to 6.3 cm no ignition occurred although resonance still occurred in the fuel line. When resonance occurred, the gases were found to have pressures and temperatures several times higher than the initial stagnation conditions. Approximate calculations by Shapiro[23] indicate that resonating gases in chambers can exceed the average temperature values by a factor of approximately 4. The measured temperatures (1100°K) are higher than those required for thermal ignition of hydrogen-oxygen mixtures. The temperatures were even sufficiently high for thermal ignition of hydrogen-air mixtures. An examination of the experimental procedure shows that autoignitions of the hydrogen-oxygen mixtures were most easily produced when the oxygen flow was stabilized first and the hydrogen flow was added later. Oxygen gas was prevented from diffusing into the fuel line by a check valve. The hydrogen line acted as resonance chamber. The oxygen gas was heated by this resonance. When hydrogen was added to the heated oxygen, ignition occurred. Ignition of hydrogen-air mixtures possibly did not occur because of their longer ignition delay times.

Schlieren photographs of the second resonant mode (Figs. 15 and 16) in a 0.95-cm-square fuel line indicate that a series of strong shock waves and wave interactions occur during each cycle of this mode. In this tube the third and most severe resonant mode did not appear. However, when fillets were placed in the corners of this square mixing tube, the third resonant mode appeared. This observation suggests that the corners influence the formation of the waves in the fuel line. The analysis of the complicated wave structure of the various resonant mode is still in progress. Also, the possibility that ignition is caused by a mechanism different from aerodynamic resonance is still under study.

REFERENCES

1. Ferri, A., "A Review of Problems in Application of Supersonic Combustion," J. Roy Aeron. Soc., 68:645, (1964), 575-597.

2. Lewis, B., and von Elbe G., Combustion, Flames and Explosions of Gases, 2nd ed. New York: Academic Press, Inc., (1961).

3. Belles, F. E., and Ehlers, J., "Shock Wave Ignition of H_2-O_2-Diluent Mixtures Near Detonation Limits," ARS Journal, 32:2 (February, 1962), 215-220.

4. Shepherd, W. C. F., "The Ignition of Gas Mixtures by Impulsive Pressures," Third Symposium on Combustion, Flame and Explosion Phenomena, Baltimore: The Williams & Wilkins Company, (1949), 301-316.

5. Kane, G. P.; Chamberlain, E. A. C.; and Townend, D. T. A., "The Spontaneous Ignition under Pressure of the Simpler Aliphatic Hydrocarbons, Alcohols, and Aldehydes," Chem. Soc. (1937), 436-443.

6. Fay, J. A., "Some Experiments on the Initiation of Detonation in $2H_2$-O_2 Mixtures by Uniform Shock Waves," Fourth Symposium (International) on Combustion. Baltimore: The Williams & Wilkins Company, (1953), 501-507.

7. Craig, R. R., "Shock Tube Study of the Ignition Delay in Hydrogen-Air Mixtures near the Second Explosion Limit," M. Sc. Thesis, The Ohio State University, Columbus, Ohio, (1966).

8. Mullaney, G. J.; Peh, S. Ku.; and Botch, W. D., "Determination of Induction Times in One-Dimensional Detonations (H_2, C_2H_2, and C_2H_4)," AIAA Journal, 3 (May, 1965), 873-875.

9. Momtchiloff, I. N.; Taback, E. D.; and Buswell, R. F., "Kinetics in Hydrogen-Air Flow Systems. I. Calculation of Ignition Delays for Hypersonic Ramjets," Ninth Symposium (International) on Combustion, New York and London: Academic Press, (1962), 220-230.

10. Bascombe, K. N., "Calculation of Ignition Delays in the Hydrogen-Air Systems," Combustion and Flame, 11 (February, 1967), 2-10.

11. Schott, G. L., and Kinsey, J. L., "Kinetic Studies of Hydroxyl Radicals in Shock Waves. II. Induction Times in the Hydrogen-Oxygen Reaction," Chem. Phys., 29:5, (November, 1958), 1177-1182.

12. Nicholls, J. A., Adamson Jr., T. C.; and Morrison, R. B., "Ignition Time Delay of Hydrogen-Oxygen-Diluent Mixtures at High Temperatures," AIAA Journal, 1.10, (October, 1963), 2253-2257.

13. McKenna, W. W., "An Investigation of the Behavior of a Detonation Wave in a Flowing Combustible Mixture," Ph.D. Dissertation, The Ohio State University, Columbus, Ohio, (1966); (also ARL 66-0112, Wright-Patterson AFB, Onio, June, 1966).

14. Hamilton, L. A., "An Experimental Investigation of Shock Initiated Detonation Waves in a Flowing Combustible Mixture," Ph.D. Dissertation, The Ohio State University, Columbus, Ohio, (1967); (also ARL 67-0202, Wright-Patterson AFB, Ohio, October, 1967).

15. Bollinger, L. E., et al., "Formation of Detonation Waves in Flowing Hydrogen-Oxygen and Methane-Oxygen Mixtures," AIAA Journal, 4: 10 (October, 1966), 1773-1776.

16. Tamango, J.; Fructman, I.; and Slutsky, S., "Supersonic Combustion in Premixed Hydrocarbon-Air Flow," GASL Technical Report No. 602, Contract No. AFOSR 66-0872, (May, 1966).

17. "Fluid Meters, Their Theory and Application, Part 1"(ASME, New York, 1937), 4th ed.

18. Liepmann, H. W., and Roshko, A., Elements of Gasdynamics, 1st ed. New York and London: John Wiley & Sons, Inc., (1957).

19. Bollinger, L. E.; Fong, M. C.; Laughrey, J. A.; and R. Edse, NASA TN D-1983, (June, 1963).

20. Steinburg, M., and Kaskan, W. E., "The Ignition of Combustible Mixtures by Shock Waves," Fifth Symposium (International) on Combustion, New York: Reinhold Publishing Corp., (1955), 664-671.

21. East, L. F., "Aerodynamic Induced Resonance in Rectangular Cavities," J. Sound and Vibrations, 3, (1966), 277-287.

22. Plumbee, H. E.; Gibson, J. S.; Lassiter, L. W., "Theoretical and Experimental Investigation of the Acoustic Response of Cavities in Aerodynamic Flow," WADC TR-61-65 (March, 1962).

23. Shapiro, A. H., "On the Maximum Attainable Temperature in Resonance Tubes," Aero/Space Sciences, 27:1 (January, 1960), 66-67.

24. Asaba, T.; Yoneda, N.; Kakihara, N.; and Hikita, T., "A Shock Tube Study of Ignition of Methane-Oxygen Mixtures," Ninth Symposium (International) on Combustion, New York and London: Academic Press, (1962), 193-200.

25. White, D. R., "Density Induction Times in Very Lean Mixtures of D_2, H_2, C_2H_2, and C_2H_4, with O_2," Eleventh Symposium (International) on Combustion, Pittsburgh: The Combustion Institute, (1967), 147-154.

APPENDIX I

COMPOSITION OF TEST GASES

Hydrogen Gas:

Manufacturer	Burdett Manufacturing Co.
Grade	Commercial
Purity	99.8%
Dew Point	-75°F
Impurities	He, N_2, O_2, CO_2, H_2O, CO

Oxygen Gas:

Manufacturer	Liquid Carbonic Co.
Grade	Commercial
Purity	99.5%
Impurities	Ar - 0.04%
	N_2 - 0.20%
	CO_2 - 20 PPM
	H_2O - 20 PPM
	CH_4 - 25 PPM

Methane Gas:

Manufacturer	Matheson Co., Inc.
Grade	Technical
Purity	97.0%
Impurities	CO_2 - 0.3%
	N_2 - 0.7%
	O_2 - 0.2%
	C_2H_6 - 1.3%
	Propane - 0.3%
	Higher Alkanes - 0.2%

Ethylene Gas:

Manufacturer	Baker and Co.
Grade	Technical
Purity	96.7%
Impurities	CH_4 - 0.9%
	C_2H_6 - 2.3%
	C_3H_8 - 0.1%
	Dew Point -50°F

Air:

Pumped at this laboratory
Dew Point -140°F
Oil - none

UNCLASSIFIED

Security Classification

DOCUMENT CONTROL DATA - R & D

(Security classification of title, body of abstract and indexing annotation must be entered when the overall report is classified)

1. ORIGINATING ACTIVITY (Corporate author)	2a. REPORT SECURITY CLASSIFICATION
Aeronautical and Astronautical Research Laboratory The Ohio State University	2b. GROUP

3. REPORT TITLE

INVESTIGATION OF THE IGNITION PROPERTIES OF FLOWING COMBUSTIBLE GAS MIXTURES

4. DESCRIPTIVE NOTES (Type of report and inclusive dates)

Final Technical Report

5. AUTHOR(S) (First name, middle initial, last name)

Walker, D. W., Diehl, L. A. Strauss W. A., Edse, R.

6. REPORT DATE	7a. TOTAL NO. OF PAGES	7b. NO. OF REFS
August 1969	58	25

8a. CONTRACT OR GRANT NO	9a. ORIGINATOR'S REPORT NUMBER(S)
F33615-68-C-1580	
b. PROJECT NO. 3012	
c. Task No. 301206	9b. OTHER REPORT NO(S) (Any other numbers that may be assigned this report)
d.	AFAPL-TR-69-82

10. DISTRIBUTION STATEMENT

This document is subject to special export controls and each transmittal to foreign governments or foreign nationals may be made only with prior approval of the Air Force Aero Propulsion Laboratory, APRT, Wright-Patterson AFB, Ohio 45433.

11. SUPPLEMENTARY NOTES	12. SPONSORING MILITARY ACTIVITY
	AFAPL AFSC Wright-Patterson AFB, Ohio 45433

13. ABSTRACT

Ignition delay times, ignition temperatures, and spontaneous ignitions were determined for several combustible gas mixtures behind incident and reflected shock waves passed into the static or flowing gases.

The conditions leading to spontaneous ignition of flowing hydrogen-oxygen mixtures without the presence of shock waves were also determined. Hydrogen air mixture did not ignite spontaneously under the range of experiments conducted.

Although certain observations indicate that the spontaneous ignition can be produced by aerodynamic heating, it must be assumed that other phenomena could also cause these ignitions. The observed high temperatures in the resonating gases should have been sufficient to ignite the hydrogen-air mixtures.

While the ignition temperature and ignition delay time of methane-air and ethylene-air mixtures do not depend on the motion of the unburned gas mixture, those of hydrogen-air mixtures were much lower behind incident than behind reflected shock waves.

A brief discussion of the mechanism of ignition under the various conditions is included.

DD FORM 1 NOV 68 1473

UNCLASSIFIED

Security Classification